MICROFLUIDIC SYSTEMS FOR STUDYING CELL MOTILITY

by

SRIKANTH VASUDEVAN

Presented to the Faculty of the Graduate School of
The University of Texas at Arlington in Partial Fulfillment
of the Requirements
for the Degree of

MASTER OF SCIENCE IN BIOMEDICAL ENGINEERING

THE UNIVERSITY OF TEXAS AT ARLINGTON
AUGUST 2010

ACKNOWLEDGEMENTS

There are many people who have helped me during my graduate education as my family, mentors, friends and colleagues. I would like to thank my mentor Dr. Young-tae Kim for considering me as a candidate for this research and guiding me throughout the project. He has been an encouragement throughout helped me in all situations. I thank him for considering me as a part of his family and helping me even in my personal life. He had trusted me since I joined his lab and taught me all the skills which I possess now. He made me evolve as a researcher by bestowing the best of the knowledge I could attain in the last two years.

I would to thank Dr. Digant P Dave, Dr. Robert Bachoo, Dr. Mario Romero-Ortega and Dr. Samir M. Iqbal who have shared their knowledge and experience in completing my research project successfully. I am grateful to Dr. Digant P Dave and Dr. Mario Romero-Ortega for serving on my thesis committee.

I would like to thank my lab mates Kailash Karthikeyan, Shreevidhya Banda, Shruti Kanakia, Neil Hall, Chetan Bhuwania and Deepika Tamuly for their technical support and inputs in my research work.

I finally thank my father Mr. A. Vasudevan, mother V. Pankaja and my siblings V. Premanand and S. Srividya for their unconditional love, faith and support throughout my achievements. I would like to thank them for laying my educational foundation and helping me throughout my life to have achieved my master's degree.

July 7, 2010

ABSTRACT

MICROFLUIDIC SYSTEMS TO STUDY

CELL MOTILITY

Srikanth Vasudevan, M.S.

The University of Texas at Arlington, 2010

Supervising Professor: Young-tae Kim

It is very imperative to develop new *in vitro* platforms that can help in studying the complex interactions that occur between cell-extracellular matrix (ECM) proteins and also during the process of cell migration *in vivo*. Such tools would facilitate in better understanding of the mechanisms that are employed by the cells during growth and migration. There are two devices presented in this study; 1) Multi-biomolecule coated lane device for unbiased cell preferential migration and 2) Novel microchannel device for real time monitoring of tumor cell migration.

The Multi-biomolecule coated lane device is an *in vitro* platform that helps in studying cell-biomolecule interaction using microfluidics systems. It provides an unbiased cell-ECM interaction with up to 20 biomolecules as compared to the commercially available techniques that restrict to 2 biomolecules at a time. The device is fabricated using Polydimethylsiloxane (PDMS), consisting of multiple protein lanes and a separate cell seeding area. Different proteins (fibronectin, laminin, collagen type 1, vitronectin, bovine serum albumin, Aggrecan) were seeded into the lanes and were allowed to be absorbed on to the substrate in cell culture incubator. Unbound proteins were washed and mammalian neuronal cells and human glioblastoma multiforme (hGBM) cells were seeded in the cell seeding area. It was seen that the

cortical neurons showed a growth towards Laminin, fibronectin, collagen type 1, vitronectin and BSA, but aggrecan inhibited the growth of axons and astrocytes. Dorsal root ganglion (DRG) and Schwann cells showed a robust growth towards the lanes containing collagen type 1, fibronectin and Laminin. The hGBM cells migrated and showed the maximum migration on laminin compared to other proteins. Migration was also observed in lanes containing collagen type1, fibronectin and BSA. This platform presented here introduces a new scientific technique to study the interaction of different cells with proteins and other biomolecules to throw light on the complex interactions occurring *in vivo.*

Novel microchannel device for real time monitoring of tumor cell migration is a microfluidic device consisting of two different microchannel patterns; (1) Taper design: with the channels tapering towards the distal end reservoir (from 20 µm, 15 µm, 10 µm, 8 µm to 5 µm) for studying single cell migration with respect to space, (2) Multichannel design: with adjacent lanes of different dimensions (20 µm, 15 µm, 10 µm, 8 µm and 5 µm). The device substrate was coated with laminin followed by seeding of primary human Glioblastoma Multiforme cells. Images were taken during the course of cell migration through the channels and were quantified for the rate of migration. The cells underwent massive morphological changes in narrow spaces and there was a significant difference in the rate of migration between the 5 µm lane and 15 µm. This serves as a new platform to understand the mechanisms involved in cancer migration with respect to availability of space and this would contribute in betterment of current treatment procedures associated with the treatment of GBM.

TABLE OF CONTENTS

LIST OF ILLUSTRATIONS

LIST OF TABLES

CHAPTER 1

INTRODUCTION

1.1 Introduction to the project

Microfluidic systems are considered as a potential platform for biological applications in the current era of research. They capacitate the study of fluid characteristics flowing through microchannels in a geometrically constrained area in μm scale [1]. The control over chemical reactions, reduced usage of expensive materials, high throughput, hyper sensitivity and high efficiency of the product yield are some of the advantages microfluidic systems [2, 3]. Polydimethylsiloxane (PDMS) based microfluidic systems are widely used for biological applications as they are bio-inert (non-toxic to cells), flexible, possess optical transparency down to 230 nm, permeable to gases but impermeable to water, easy to fabricate and can be bonded to other surfaces. Some of the biological applications are cell culture, cell sorting, cell counting, polymerase chain reaction (PCR), DNA sequencing, DNA separation and immunoassays [4-6]. Microfluidic devices have been extensively used for studying neuronal growth and regeneration by isolating axons from somata and dendrites into microchannels [7, 8]. Complications of PDMS based microfluidic devices is surface hydrophobicity [9] with a contact angle 104°-120°[10] due to the presence of CH_3 in the repeating -0Si(CH_3)- groups. Hydrophylicity of PDMS surface is achieved by using air plasma or corona treatments [11], which oxidizes the surface to silanol (Si-OH). Constant contact with water keeps the surface hydrophilic and 30 minute exposure to air brings the hydrophobic groups to re-surface, lowering the surface free energy [4, 12, 13]. The microfluidic devices are kept in contact with liquids constantly for biological applications and this enable to retain hydrophilicity. Some applications of PDMS based microfluidic systems are shown in figure 1.1. All these characteristic features make microfluidic systems a suitable candidate for pursuing biological research.

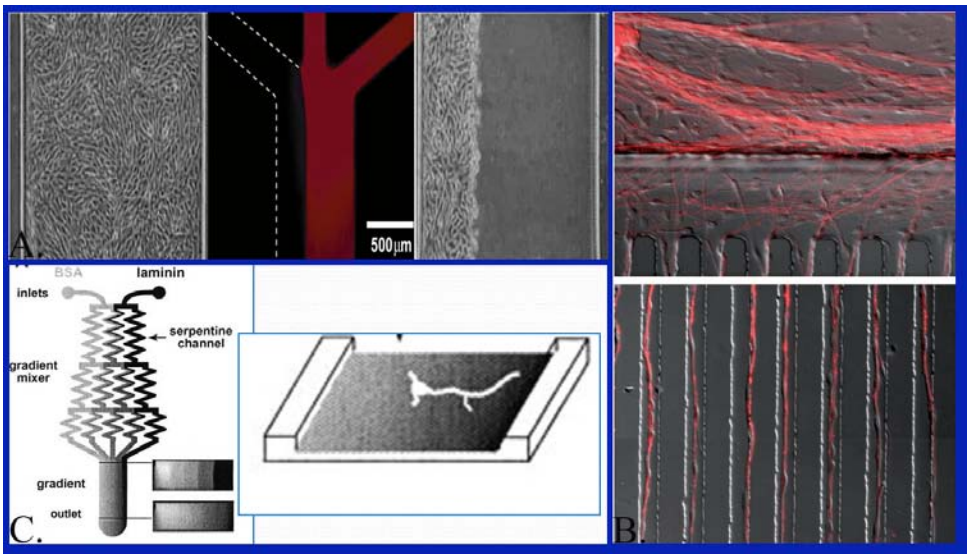

Figure 1.1 Biological applications of microfluidic devices. (A) Wound assays using laminar flow [14] (B) Axonal isolation study [8] (C) Effect of protein gradient on mammalian neurons [15].

Microfluidic chips are employed in studying the mechanism that underlies the growth and migration of cells *in vitro.* These cellular processes are controlled by the interaction with the micro-environment and signals that guide them [16]. Studies reveal diverse molecules that regulate the development of cells in the nervous system like trophic factors, cell adhesion molecules (NCAM, L1, NgCAM) and extracellular matrix (ECM) proteins [17-19]. Some common ECM proteins found in the body like laminin, fibronectin, collagen, aggrecan, vitronectin [20-23] are involved in growth and development. ECM is a complex mixture of macromolecules like proteoglycans, structural proteins and specialized proteins [24, 25], that govern the growth, development and motility of neurons and glial cells [26, 27]. The accuracy of axon innervations during development of the nervous system is controlled by axon growth cone steering, for which one of the main guidance cues is ECM. The growth cone forms stable adhesion with the matrix proteins leading to accumulation of F-actin at the leading end [28, 29]. ECM also renders support for malignant tumors during invasion and metastasis [30]. ECM signaling plays a major role ranging from developmental abnormalities to cancer development [31]. During surgical excision of brain tumor, neoplastic cells that infiltrate the adjacent normal brain cannot be removed

completely leading to recurrence of tumor after surgical intervention [32, 33]. The process of cancer cell migration is mainly dependent upon the substrate formed by ECM, which help cell attachment as well as acts as a barrier for advancement of the cell body. The cells modify morphology and develop protruding processes in the leading end which contains actin and other proteins like integrins to form focal adhesion with substrate which help in exerting force to move towards the proceeding end [34, 35]. Thus, it is imperative to study the interaction of cells with individual components of the ECM *in vitro* to understand process that occurs *in vivo.* A microfluidic device is proposed to study the interaction of cells with multiple biomolecules *in vitro*, called multi-biomolecule coated lane device.

Glioblastoma Multiforme (GBM) is a highly invasive and aggressive primary brain tumor found with a median life expectancy of less than 1 year from the time of diagnosis [36 37]. The rate of survival despite surgical removal, radiotherapy and chemotherapy for the treatment of GBM has not increased the rate of survival [38]. Tumor cell migration to the normal surrounding areas of the brain is a key factor for evading successful treatment [34]. Pharmacological intervention to arrest migration is considered for achieving better treatment outcome for GBM [39-41]. GBM is subjected to destruction by immune system outside central nervous system (CNS), the basement membrane of the blood vessels inhibits intravascular access and it is found that GBM rarely cross the blood brain barrier [42, 43]. Brain tumor cells migrate using critical cell adhesion molecules (CAM) known as integrins. Integrins are heterodimers with α and β subunits found on the cell surface. Coordinated interactions of integrins with the three amino acid sequences RGD (Arg-Gly-Asp) found in many of the ECM proteins forms a complex of ECM-integrin-cytoskeleton which help during invasion and cell migration [44, 45]. During this process, a cell modifies its shape and stiffness leading to change in cell morphology [46]. The polarization of the cell leads to protrusion of psuedopods at the leading edge which contact the adjacent ECM and bind with the help of integrins and facilitate cell motility [35]. This change in cell morphology is influenced by availability of space and cellular environment in the region, which is complicated

to study *in vivo*. *In vitro* studies help understand the internal and external signals that facilitate the change in tumor cell morphology, but the cells are given enormous space unlike the extracellular space of the body, which is in sub-micron scale [47] [48]. Thus, developing newer techniques to improve *in vitro* studies for understanding these behaviors exhibited by the GBM or any other cancerous cell *in vivo* is important. Even though getting coordinates similar to *in vivo* conditions is inconceivable, devices that would pose the cells with space constrictions are feasible *in vitro*. Researchers have shown that the cell migration is influenced by the topography of surrounding environment [49, 50]. Cancer cells re-organize their cytoskeleton and can migrate through narrow spaces in the presence of micro-patterns which control their migration [51, 52]. To study these characteristics of GBM, two microfluidic devices are proposed in this project that pose cells with space constrictions. The devices are called (1) Novel microchannel device- taper design and (2) Novel microchannel device-multichannel design.

1.1.1 Fabrication of microfluidic devices

Mask with patterns were designed using AutoCAD and transferred to a silicon wafer using soft lithography. The silicon wafer along with the polymerized photoresist served as the master mold for fabricating microfluidic devices. Polydimethylsiloxane (PDMS) was poured onto the master mold and cured to form PDMS based microfluidic devices.

1.1.2 Extraction of primary neurons

Timed pregnant Sprague Dawley (SD) rats were used for collecting primary neuronal cells. Cortical neurons and dorsal root ganglion (DRG) neurons were collected from embryonic day E-18 embryos. Cells were harvested and dissociated to obtain individual cells and seeded into the microfluidic devices and cultured in Neurobasal Medium + B-27 at 37°C, 5% CO_2 during the course of experiment.

1.1.3 Primary human Glioblastoma Multiforme cell culture

hGBM cells were isolated with consent from patients at The University of Texas Southwesterm Medical Center (Dallas, TX) with approval of institutional review board. The cells

were dissociated chemically and cultured in serum free DMEM/F-12 + B-27 medium and used for studies in microfluidic devices.

1.1.4 Cell migration study in multi-biomolecule device

Multiple ECM proteins were used to study cell-biomolecule interactions. Proteins were allowed to adsorb on to the substrate and unbound proteins were washed. The cells were placed in an isolated cell seeding area. Markers were used to find out the location of the protein lanes. Once the cells attached to the substrate and grew processes, the device was peeled off and the cell migration towards different ECM proteins was studied.

1.1.5 Cell migration study in microchannel device

The devices were assembled on glass coverslips followed by laminin coating to support adhesion and growth of hGBM cells. Cells were seeded in the proximal side reservoir and allowed to migrate through the microchannels. Images were taken during cell migration through the microchannels for evaluating the change in cell morphology.

1.2 Background and significance

1.2.1 Studying cell-biomolecule interaction in vitro

The current major techniques to study the cell-biomolecule interactions are performed by using a protein coated substrate or two alternate protein coated stripes designed by F. Bonhoeffer and group to study the axonal guidance mechanisms *in vitro* [16, 53]. Using protein coated substrates, the effect of ECM proteins (laminin, fibronectin) on the cells is studied while cells grown on them [54, 55]. The original stripe assays were formed by drawing crude tissue fractions or transfected guidance molecules with the help of vacuum into the striped pattern. This lead to the discovery of graded distribution of axon repulsive molecules in the posterior tectal membranes of the chick retino-tectal system [56, 57]. The stripe assay also lead to the discovery of ephrin-As to be responsible for the repulsive properties [58, 59]. The current versions of stripe assays are fabricated using special silicone matrices and the substrate preferences are left to the experimenter. Alternate stripes are formed by coating one set of stripes and filling the

gap in between to form the second set of stripes. Laminin is spread homogenously to facilitate cell attachment [60]. The drawback of current systems if that the reduced efficiency (maximum 2 biomolecules at a time), cells do not confront the proteins as seen *in vivo* and the proteins in stripe assays are not pure leading to mixed results [61]. There are improved stripe assays which give pure proteins and where the cells face the interface of proteins, but they are limited to 2 proteins at a time.

Although the techniques are well established and set a standard for studying cell-biomolecule interactions, a maximum of 2 biomolecules can be studied simultaneously. Proteins in the stripe assays are not pure and give mixed results when using aggrecan and laminin [61]. The cells confront the proteins *in vivo* and refrain to growth through inhibitory molecules [62]. Studies mentioned here are performed by seeding cells on top of the proteins. To address this issue, we have developed an *in vitro* microfluidic platform to study the cell-biomolecule interaction with up to 20 pure biomolecules simultaneously. Stripes of different proteins are formed and the cells show growth or repulsive behavior towards the confronting ECM proteins.

1.2.2 Studying tumor cell migration in vitro

There are two major types of *in vitro* tumor cell migration studies, 2-D and 3-D assays. The complexity of the 2-D assays is arbitrary migration quantification, microfluidic channels that do not pose the space constrictions and inability to replicate the *in vivo* environment like chemical gradients. Although the 3-D assays imitate the *in vivo* environment, real time quantification is limited. The limited choice for membrane materials in 3-D complicate the studying of cell-cell, cell-ECM or morphogenesis within the ECM [63]. Microfluidic systems are being developed for 2-D and 3-D assays in recent years [64]. Boyden chamber assay is an approach to study the process of cell migration through narrow pores. There are two chambers one on top of the other separated by a polycarbonate membrane with pores of definite diameters (0.1 – 20 μm). ECM is coated to mimic basal lamina and cells are seeded in the top chamber. After a few hours, the cells proteolysis of ECM proteins and migrate through the

porous membrane towards the bottom chamber as the cells are attracted due to the presence of chemoattractants in the bottom chamber. Migrated cells are quantified and the molecules involved at the focal adhesion is studied by histology. This process is related to migration of cells into the blood stream during metastasis [65, 66]. GBM migration rate *in vivo* is calculated by obtaining two pre-treatment MRI images to study proliferation and invasion of these cells [67, 68].The complexity of studying cell migration real time and the short migration duration in Boyden's chamber assay (membrane thickness of 6-10 μm) necessitates the need for newer platforms to study cancer cell migration real time over larger distances.

We introduce two microfluidic devices with different microchannel designs to study migration of cancer cells in restricted space. The designs were made keeping in mind the ability of cancer cells to remarkably deform their cell shape to squeeze through narrow spaces during migration [51]. The devices are named after the channel design as:(1) Taper design- the channels taper from the gradually over fixed distance (from 20um, 15um, 10um, 8um to 5um), (2) Multichannel design- the channels of 20um, 15um, 10um, 8um and 5um width are arranged adjacent to each other.

The cells are seeded in the proximal end reservoir and studied morphologically during the course of migration towards the distal end reservoir. The taper design enables one single cell to change morphology while travelling towards the distal end reservoir, forcing the cells to use intracellular mechanisms to overcome space constrictions during migration. The multichannel design is used to study the rate of migration of cells with respect to space over longer distances to calculate the migration rate and compare the effects of channel dimension (topography) on migration. Such a study would impart more knowledge on the mechanisms involved by cancer cells during migration in geometrically constricted areas and would support in betterment of treatment associated with tumor migration and metastasis.

1.3 The Nervous System

The nervous system is classified into central nervous system (CNS) consisting of brain and spinal cord and the peripheral nervous system (PNS) connecting the CNS to the peripheral organs for sensory and motor functions. Neurons and glial cells (CNS: astrocytes, oligodendrocytes, microglia, ependymal cells ; PNS: Schwann cells, satellite cells, enteric glial cells) [69, 70] are building blocks of the nervous system. Neurons were first discovered by Santiago Ramón Cajal for which he was awarded a Nobel Prize [71]. Neurons are electrically active and the primary mode of communication is using electrical communication called action potentials (AP). Glail cells outnumber the neurons (1:10, Neurons: Glial cells) in developed nervous system and play vital roles like support, guidance, chemical regulation, conduction of AP during development and normal functioning of nervous system [72].

Brain is made up of several types of neurons working in synchrony. The cerebral cortex is the layer consisting of cell bodies (grey matter) forming the top layers of the cerebral hemispheres. It is made up of six layers that receive inputs from different regions of the brain and form connection with other regions to evoke responses [73, 74]. Cortical neurons receive input from corresponding areas in the periphery for which they evoke a response [75]. Damage in the cerebral cortex leads to lack of bodily functions, which necessitates their study that can lead to improvisation of current treatment methods and contribute to their regeneration.

Neurons of PNS called dorsal root ganglion (DRG) cells are the primary sensory neurons that give input to the CNS by forming synaptic junctions inside the spinal cord. They are psuedounipolar cells that project their axons to the sensory organs and the other end forms synaptic inputs with the spinal cord [76]. Damage to peripheral nerves causes lack of sensory and motor functions.

1.4 Glioblastoma Multiforme

Gliomas are neoplasms found in central nervous system (CNS) and comprise 60% of all CNS malignancies. They are classified into astrocytomas and oligodendrogliomas depending on the resemblances between the normal glial cells and the malignancies. Astrocytomas are the most common gliomas and Glioblastoma Multiforme (GBM) is the most aggressive form of astrocytomas. World Health Organization (WHO) grade IV is the most malignant and the most common Glioblastoma constituting 15 – 20% of all primary intracranial tumors. The median survival rate after maximum treatment still remains between 12 -18 months with few cases of long term survival. GBM diagnosis and surgical guidance is performed using MRI imaging [67]. Despite surgery, radiotherapy and chemotherapy, GBM recurs leading to patient mortality. So far, there has been no significant treatment outcome from the current methods of treatment for GBM [77-80].

Gliomas have spindle shaped morphology similar to fibroblasts and their adhesion is dependent on integrins [35]. They have high traction forces found on both poles found in the cell [35]. They tend to migrate as a single cell from a colony of cells and the major problem associated with the treatment of hGBM is that they migrate and infiltrate into the normal surrounding areas of the brain and evade the treatment [34, 81]. GBM recurrence is observed close to the area of resection and recurrence >2cm from the site is uncommon [82, 83]. Methylating agent Temozolomide (TMZ) is the most effective chemotherapeutic agent considered for GBM treatment to which, drug resistance is modulated by O(6)-methylguanine-DNA methyltransferace (MGMT), a DNA repair protein [84-86]. GBM tend to undergo morphological changes during migration within extracellular spaces [87] which is attributed to chloride channel mediated fluid secretion [88, 89]. Under spatial constrictions, migrating GBM cells undergo rearrangement of cytoskeleton to support change in volume and shape [90]. Arresting GBM migration is considered for better treatment [82, 91] outcome requiring platforms for studying GBM migration *in vitro*.

1.5 Objective of the Research Project

The objective of this project is to introduce *in vitro* microfluidic platforms that can be used to study the cell-biomolecule interactions and cell migration with respect to space constrictions encountered by cells *in vivo*. The specific aims are:

1. To study cell interaction with multiple confronting biomolecules *in vitro.*
2. To introduce space constrictions to migrating GBM cells to induce morphological changes.

CHAPTER 2

FABRICATION AND ASSEMBLY OF MICROFLUIDIC DEVICES

2.1 Designing of mask for soft lithography

The mask serves as the cover to transfer the designed pattern on to photoresist coated silicon wafer that would act as mold for fabricating microfluidic devices using Polydimethylsiloxane (PDMS). The desired dimension of the patterns is designed using AutoCAD and sent for fabrication of mask. Mylar mask is made for the multi-biomolecule device and for achieving high resolution for microchannel device, a chrome mask is fabricated. The multi-biomolecule device is a single layer process with minimum dimension of 50 µm, which can be achieved by direct mylar mask printing. The design consists of multiple protein lanes of 100 µm width and reservoirs connecting either ends of the lanes. The cell seeding area is separated from the lanes by a distance of 50 µm for getting the cells as close as possible to the protein lanes. The microchannel device has a minimum dimension of 5 µm which is achieved by using chrome masks. The device is a dual layer process, one layer consisting of channels (15µm high) and the other layer consisting of reservoirs (100 µm high) connecting the channels on either sides. This helps in achieving two different heights, one for the channels and the other for reservoirs.

2.2 Silicon master mold preparation

All steps were performed in Nanofabrication center at The University of Texas at Arlington.

Materials: 4” Silicone wafer (Wafer world), Photoresist: SU-8 5, SU-8 50 (MicroChem), SU-8 developer (MicroChem), Spin coater, Backside aligner, hot plates, Acetone and Isopropyl alcohol.

Step 1 - Substrate pre-treatment: The substrate of the silicon wafer was cleaned with solvent (Acetone) followed by DI (18.2 MΩ) water rinse to obtain maximum process reliability. Wafer was dehydrated at 200 °C for 10 minutes on a hot plate to remove any adsorbed moisture content.

Critical step: Ensure dehydration of wafer to avoid problems with adhesion of photoresist.

Step 2 - Spin coating photoresist on wafer: Approximately 1 ml resist per inch of wafer is used. The process of spinning was done in two steps by gradually increasing the speed fromstep 1 to step 2 to achieve even coating. The spin coated photoresist determines the effective height of the pattern to be formed.

15 µm height: Resist SU-8 5

(1) 500 rpm at 100 rpm/sec for 5 seconds.

(2) 1000 rpm at 300 rpm/sec for 30 seconds.

100 µm height: Resist SU-8 50

(1) 500 rpm at 100 rpm/sec for 10 seconds.

(2) 1000 rpm at 300 rpm/sec for 30 seconds.

Step 3 - Soft baking of the photoresist: The wafer is baked after the resist is spin coated in order to evaporate the solvent and to make the resist film dense. The bake temperatures of 65 °C and 95 °C are constant with change in baking time depending on the viscosity of photoresist and height of the desired pattern.

15 µm height: 2 minutes at 65 °C and 5 minutes at 95 °C.

100 µm height: 10 minutes at 65 °C and 30 minutes at 95°C.

Step 4 - Exposing the photoresist to UV through mask to form pattern: The SU-8 resist used in the process is optimized to work for near UV (350 – 400 nm) wavelength. The exposure energy used is between 300 mJ/cm2 – 550 mJ/cm^2. Upon exposure, the negative photoresist cross links leaving the pattern area to be polymerized. The time of exposure to cross link the resist is used as per the manufacturer's recommendations.

15 µm height: Single exposure for 12 seconds.

100 µm height: Two consecutive exposures for 14 seconds.

Step 5 - Post Exposure Baking (PEB): To selectively cross-link the exposed regions of the photoresist, the wafer was heated in a two step process to minimize the damage to the pattern. The temperatures are 65 °C and 95 °C and the time of baking varies with respect to pattern.

15 µm height: 1 minute at 65 °C and 2 minutes at 95°C.

100 µm height: 1 minute at 65 °C and 10 minutes at 95°C.

Step 6 - Developing the pattern: SU-8 developer is used to remove the enexposed areas in the wafer. Immersion technique was employed with wafer to clean the unexposed regions of the photoresist. This process was followed by rinsing with IPA and nitrogen blow drying.

15 µm height: 3 minute wash using SU -8 developer.

100 µm height: 10 minute wash using su-8 developer.

Step 7 - Hard baking of the wafer with pattern: For achieving maximum yield of the photoresist, the device was baked at 200 °C on a hot plate for 30 minutes before using it to fabricate microfluidic devices.

Two layer photolithography processes are performed to achieve two different pattern heights in a single pattern. It is fabricated by patterning the design with lower height first followed by aligning the second pattern with higher height on top. Figure 2.1 is a schematic representation of the process of photolithography and the procedure for obtaining microfluidic devices using the fabricated silicon wafer with patters.

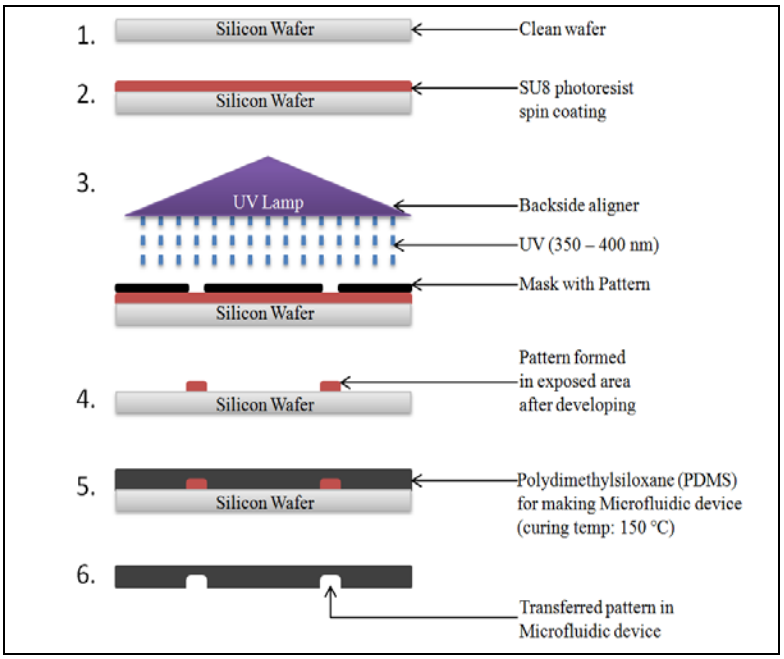

Figure 2.1 Schematic representation of photolithography and microfluidic device fabrication.

2.3 Fabrication of Microfluidic devices using PDMS

Materials: Silicon wafer with patterns, SYLGARD® 184 elastomer kit (DowCorning), vacuum dessicator, hot plates, aluminum foil and scalpel blades.

Step 1 - Mix PDMS polymer and curing agent in the ratio of 10:1 (30 ml : 3 ml) respectively and place it in vacuum dessicator (20 in Hg Vacuum) for 45 minutes. This would remove all the air bubbles caused during mixing process.

Critical step: Ensure there are no air bubbles in the mixture before removing it from the dessicator. If there are air bubbles, leave it for some more time till all air bubbles are completely removed.

Step 2 - Place the silicon wafer in aluminum foil as shown in figure 2.2 B and pour the clear PDMS mixture and place it at 150 °C for 5 minutes.

Step 3 - Remove the wafer once the PDMS cures completely and place it at 70 °C for cutting the device pattern from it as seen in figure 2.2 C.

Note: By not changing the wafer temperature abruptly from 150 °C to room temperature, the yield from a wafer can be increased. This is due to the difference in temperature of expansion of silicon wafer and photoresist.

By following the protocol mentioned above, we obtained a device height of 3.95 ± 0.2 mm and the yield from one wafer was > 25.

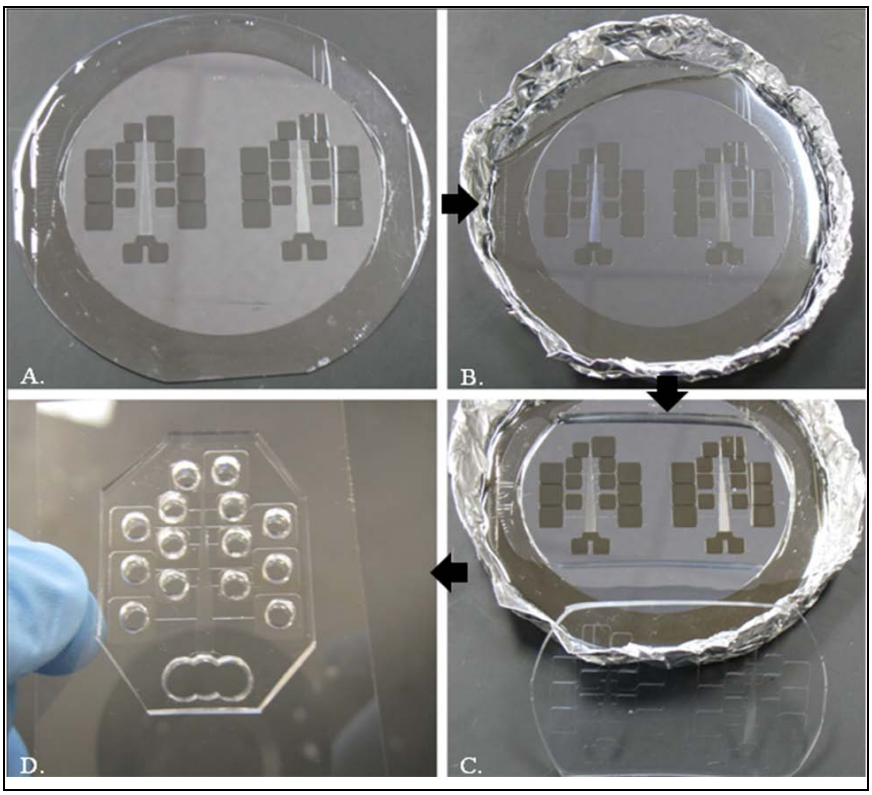

Figure 2.2 Process of microfluidic device fabrication. (A) Silicone wafer with patterns of photoresist. (B) Mixture of PDMS polymer and curing agent poured on wafer covered using aluminum foil to form boundary. (C) Cutting of device from the wafer after curing of PDMS. (D) Reservoirs of device opened using biopsy punches and placed on glass coverslip.

2.4 Assembly of microfluidic devices on substrate

Step 1 - Place the device of a flat surface and using a tissue biopsy punch, remove the PDMS to form reservoirs as seen in figure 2.2 D.

Step 2 - Clean the punched device using clear tape to remove any debris followed by inspecting it under a microscope.

Critical step: Ensure that all debris of PDMS is completely removed to avoid lifting of devices from the substrate. This would lead to leakage lead to leakage during experiments.

Step 3 - Sterilization of devices: Immerse the devices in 70% ethanol and place it inside bio-safety cabinet for 25 minutes. Remove the devices from ethanol and place it in sterile DI water (18.2 MΩ) three times with 10 minute time intervals and air dry.

Place the sterile microfluidic devices on clean substrate for pursuing experiments.

2.5 Results and Discussions

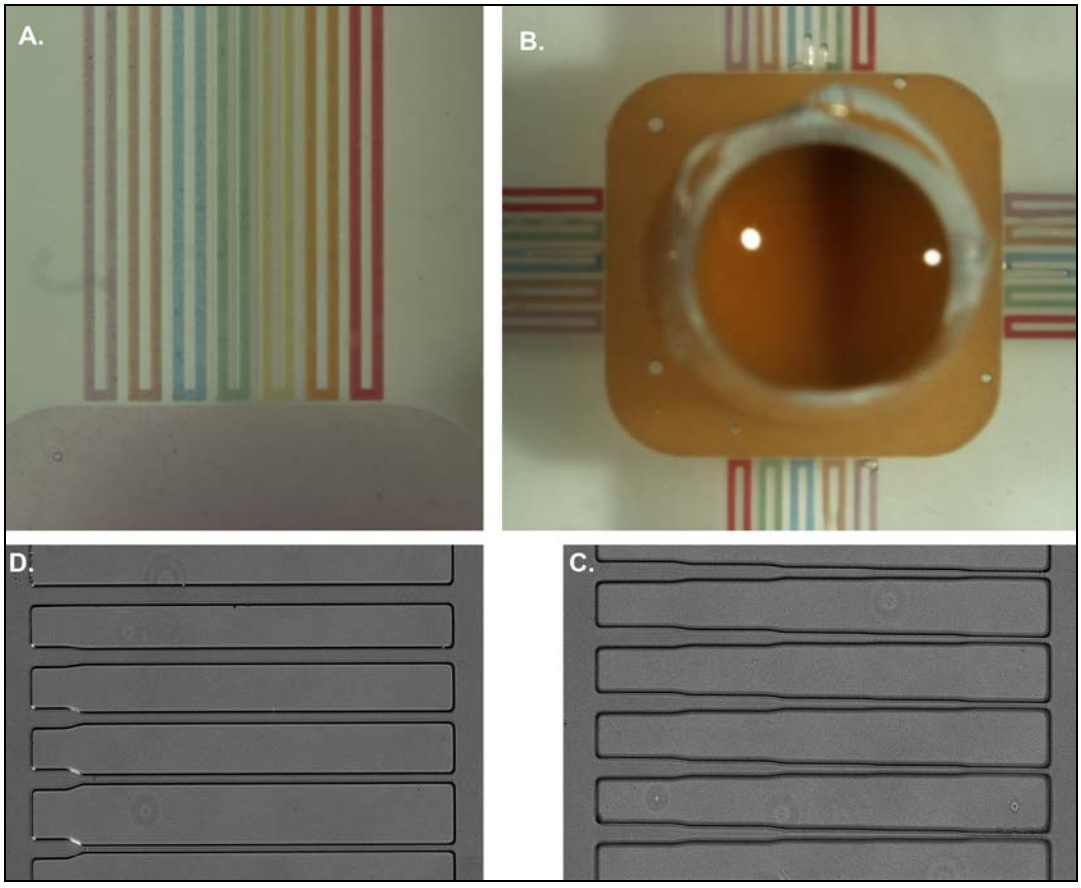

Figure 2.3 (A) Multi-biomolecule device with 7 lanes and cell seeding area shown using water colour. (B) Multi-biomolecule device with 20 lanes and cell seeding area shown using water colour. (C) Taper channels of novel multichannel device. (D) Multi-lane channels of novel multichannel device.

The masks were designed as per specifications and the wafer for Multi-biomolecule device was fabricated at a height of 100 µm using a single layer photolithography process as described. The microchannel devices were fabricated using two layer photolithography processes with the channels at a height of 15 µm and the reservoir at a height of 100 µm. Figure 2.2 shows the patterns formed in microfluidic devices using the process of photolithography. Images A and B are made 100 µm and the channels shown in images C and D are 15 µm high.

It was found that during the process of fabrication, wafer cleaning with acetone and DI water removed particles from the surface and dehydration at 200 °C for 10 minutes removed any adsorbed moisture from the silicon surface. This enhanced the adhesion of photoresist to the wafer for better process stability. Soft baking process was very crucial to remove the solvent from the photoresist in order to obtain desired patterns formed after getting dense resist.

UV exposure in multi-biomolecule device was maintained at 2 bursts of 14 seconds to ensure that the PDMS barrier between the cell seeding area and the protein lanes do not merge. Overexposure leads to change in dimensions of the patterns formed and small dimensions tend to merge leaving no PDMS walls in the device. By using the process for making 100 µm, clear patterns and reproducibility of devices were achieved.

The devices were fabricated using PDMS at 150 °C for 5 minutes per yield. During the removal of formed device from the wafer, the wafer temperature was maintained at 70 °C to avoid cooling down of the resist temperature abruptly. This enhanced the quality and yield of devices formed from the process. The yield from a wafer was >25.

CHAPER 3

MULTI-BIOMOLECULE DEVICE – DESIGN AND WORKING

3.1 Device Design Criteria

There are three major criteria to be considered for achieving preferential migration towards multi-biomolecule coated lanes on the microfluidic device:

1. Inlet and outlet reservoirs connecting individual lanes for coating and washing the unbound proteins from lanes.
2. Biomolecule coated lanes should be close to each other for cells to access proteins in the adjacent lanes.
3. Cell seeding area should be close to all the protein lanes and also should prevent the cells from entering the lanes before removing the device from the substrate

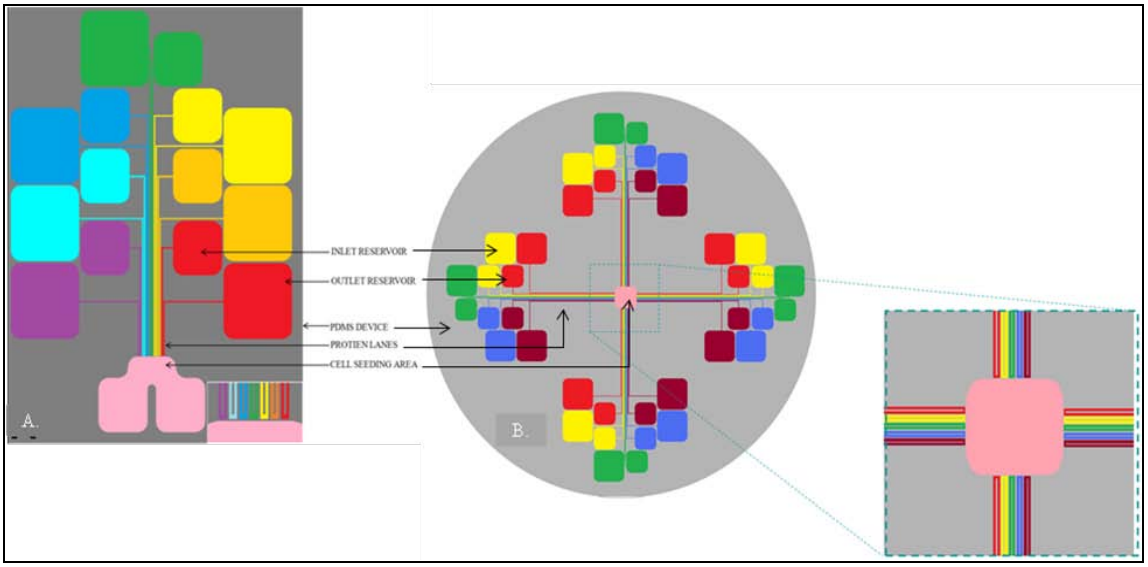

Figure 3.1 Schematic representation of (A) 7 Lane multi-biolomoleculte device (B) 20 lane multi-biomolecule device.

3.2 Dimensions of multi-biomolecule device

The inlet reservoirs are 7 X 7 mm and the outlet reservoir is 5 X 5 mm. the cell seeding area is designed to create reservoirs using 6 mm biopsy punches. The protein lanes are 28,500 µm at the longest lane and 5000 µm at the shortest lane in the 7 lane device. The 20 lanes multi-biomolecule device is 35,500 µm at the longest lane and 19,800 µm at the shortest lane.

3.3 Preparation of multi-biomolecule device

Step 1 - The inlet and outlet reservoirs are punched open using 4 mm tissue biopsy punches. The maximum amount of liquid that can be used is 70 µl per reservoir.

Step 2 - The cell seeding area is punched open using 6 mm tissue biopsy punch as shown if figure 2.2 D.

Critical step: To achieve high cell density near the PDMS barrier between cell seeding area and protein lanes, punch the cell seeding area near to the PDMS barrier.

Step 3 - The devices are cleaned and sterilized as described in section 2.5 and placed onto a 60 mm tissue culture treated Petri dish (Corning) with pattern side facing the substrate inside a bio-safety cabinet to ensure sterility.

3.4 Multi-biomolecule coating on the lanes and cell seeding

Step 1 - Mark the Petri dish from the bottom to identify the position of protein lanes and cell seeding area using permanent marker.

Step 2 - Fill 50 µl of proteins in the inlet reservoir and using the blunt end of 1000 µl micropipette (sterilized using 70% IPA), draw the proteins to the outlet reservoir using negative pressure. Fill the cell seeding area with proteins to enhance cell adhesion to substrate.

Proteins used: BSA (fluorescently tagged - green, 50 µg/ml), BSA (50 µg/ml), collagen type 1 (50 µg/ml), Laminin (10 µg/ml), fibronectin (10 µg/ml) and vitronectin (10 µg/ml), Aggrecan (500 µg/ml). All protein lanes are selected at random inside the device.

Step 3 - Place the device with protein inside cell culture incubator (37°C, 5% CO_2) for 3 - 6 hr. After protein adsorption, remove the unbound proteins from reservoirs and fill 70 µl of sterile 1X

PBS in the inlet reservoir and 20 µl 1X PBS in the outlet reservoir and leave it for 30 minutes. Repeat this process 4 times to remove all unbound proteins. Simultaneously, wash the proteins from the cell seeding area with 1X PBS.

Note: By filling the inlet and outlet reservoir with different volumes of 1X PBS, a gradient is formed allowing the 1X PBS flow from inlet to outlet. This washes off all unbound proteins from inside the protein lanes.

Step 4 - After the unbound proteins are washed, the inlet and outlet reservoirs are filled with 70 µl of 1XPBS and cell seeding area is filled with respective cell culture medium followed by cell seeding.

Step 5 - Once the cells firmly attach and grow processes, PBS from inlet and outlet reservoir is removed and the area surrounding the device is filled with medium and an "L" bent 23 gauge needle is inserted near the cell seeding area to allow diffusion of medium inside the device. Slowly, the device is lifted off and the Petri dishes are filled with medium to allow cell growth towards protein lanes.

Critical step: By draining the medium from the cell seeding area and pealing the device, there is a shear force created that leads to cell death. To avoid this, allow the medium from the surrounding to diffuse slowly as described above.

Images of cell migration are taken as the cells migrate towards the protein lanes. The device design and illustration of the procedures can be seen in figure 3.1 and 3.2. To ensure proteins in the lanes are mixed with surrounding protein lanes, BSA (green and red) were used in alternate lanes and BSA (red) was used in cell seeding area as shown in figure 3.3. This experiment was performed 7 times and it was found that all the devices had pure proteins adsorbed in the defined areas.

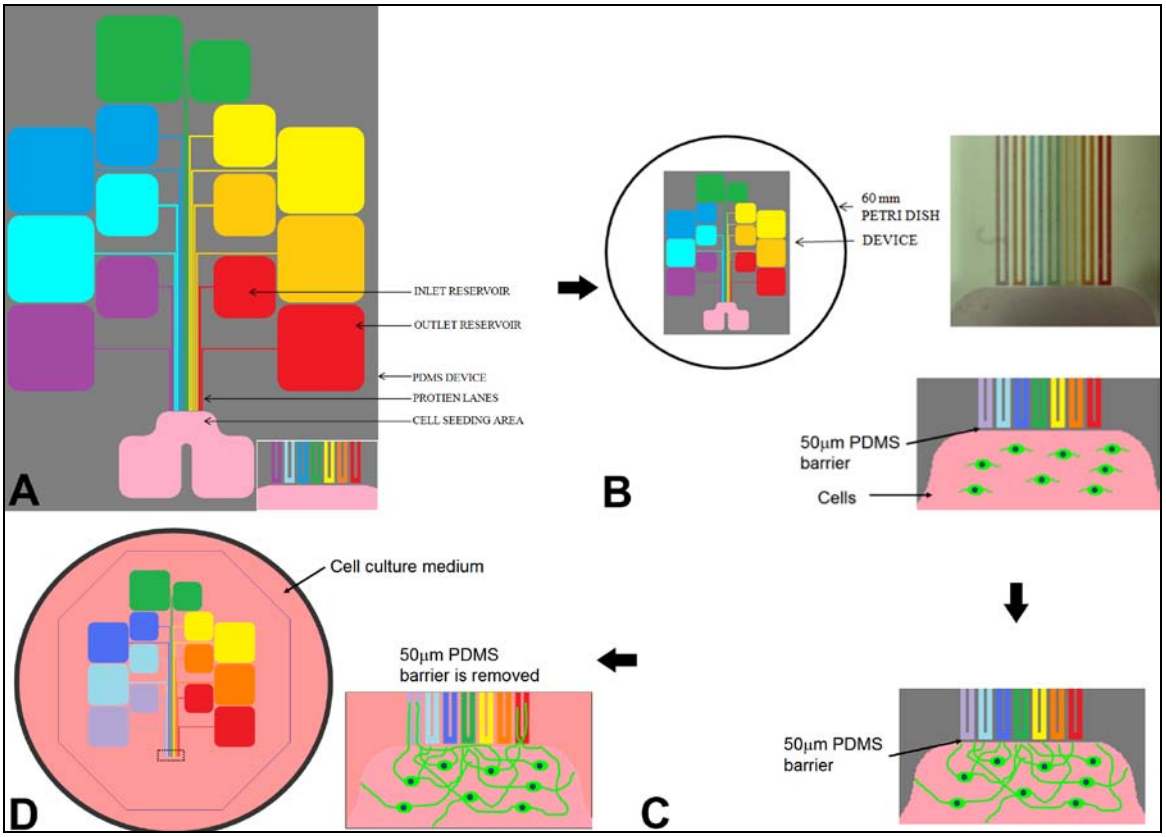

Figure 3.2 Schematic representations of Multi-Biomolecule device design and working. (A) Image showing the Multi-Biomolecule device. (B) Image showing protein coated lanes separated from cell seeding area by PDMS barrier. (C) Image showing the formation of cell processes at the interface after cell maturation. (D) Image showing cell growing towards different protein lanes after removal of PDMS device.

Figure 3.3 Alternate stripes of BSA (red and green) coated in 7 lane multi-biomolecule device. Cell seeding area is coated with BSA (red) to show the cell seeding area is separated at an equal distance from the protein lanes after removing the device.

3.5 E-18 rat embryo derived cortical neuron harvesting and seeding

All procedures were conducted according to IACUC (Institutional Animal Care and Use Committee) approved protocols.

The cortical tissues were dissected, cleaned and enzymatically digested with 0.25% trypsin for 20 minutes. The tissue was subjected to trituration using fire polished pipette and the resulting cell suspension was used for seeding cells. The cell seeding are was treated with Poly-D-Lysine (PDL) and 250,000 – 300,000 cells of cortical neurons were seeded in the cell seeding area of the multi-biomolecule device.

3.6 E-18 rat embryo derived DRG neuron and Schwann cell harvesting and seeding

Individual ganglia was removed from the spinal column and were subjected to enzymatic dissociation using 0.25% trypsin for 20 minutes followed by trituration using a fire polished pipette tip. The resulting cell suspension containing DRG and Schwann cells were seeded in the cell seeding area (coated with collagen type 1).

3.7 Primary human Glioblastoma Multiforme (hGBM) collection and seeding

hGBM samples were obtained from consenting patients at The University of Texas Southwestern Medical Center (Dallas, TX) with the Institutional Review Board approval. The cells were chemically dissociated with 2% papain and 2% dispase followed by trituration. The cells were suspended in serum free Dulbecco's modified Eagle's medium/F-12 medium, containing 2% B-27 supplement, 0.25 % Insulin-Transferin-Selenium-X, Penicilin-Streptomycin (100 units/ml and 100 µg/ml respectively) and 20 ng/ml mouse EGF. The cells were transduced with lentivirus expressing monomeric-cherry (*m-cherry*) fluorescent protein.

The cells floating in the medium were used to cell seeding. The medium was centrifuged at 1000 rpm for 5 mins. The pellet was chemically dissociated with 1 ml Trypsin-EDTA + 0.2% collagenase type II for 5 minutes at 37 °C. SBTI was added and the cells were physically triturated and centrifuged at 1000 rpm for 5 minutes. 30,000 cells from the cell pellet

were used in the cell seeding area containing DMEM/F-12 + B-27 and mEGF. In this study, the substrate was pre-treated with BSA to support adhesion of hGBM cells.

3.8 Results and Discussion

All the experiments were performed with n=6 per experiment.

3.8.1 Cortical neuron migration study

Cortical neurons derived from E-18 derived rats were used in this study. 250,000 – 300,000 cells were seeded in the cell seeding area and cultured till they formed the boundary near the PDMS wall between the proteins and cell seeding area as shown in figure 3.3 A. NBM +B-27 containing BDNF and NT-3 were used for culturing the cells. Growth factors BDNF and NT-3 contribute towards neuroprotection [92]. Cells were allowed to grow till they reach and migrate onto the protein lanes and were fixed with 4% paraformaldehyde. Axon growth on protein lanes are shown in figure 3.4 and 3.5 (stained for β-III tubulin and GFAP).

In a comparative experiment, a stripe of aggrecan (500 µg/ml) was coated on a Petri dish surface and E-18 derived cortical neurons were seeded on top of Aggrecan. The cells attached on the surface and extended neurons as shown in figure 3.4 D. The staining for astrocytes as shown in figure 3.5 indicated that the astrocytes and cortical neurons move in a co-localized manner. This shows that the migration of the cortical neurons towards the ECM proteins is also contributed by the presence of astrocytes in the culture.

The study shows that the axons and astrocytes migrated towards all the protein lanes except the lane coated with aggrecan. The growth promotion can be clearly seen in Laminin, fibronectin, vitronectin and collagen type 1 from figure 3.4 and 3.5. BSA supported less growth as compared to the other four proteins mentioned. Aggrecan had an inhibitory effect that is seen as the cells are not growing over the lane coated with aggrecan. Comparing figure 3.4 B and 3.4 D, it can be concluded that the cells when seeded on top of the proteins might show different properties compared to growing towards proteins in front like in multi-biomolecule device. This device relates to the *in vivo* conditions where the cells are confronted with inhibitory molecules

and refrain to grow through them [62]. The cortical neurons took approximately 14 days to start migrating towards the protein lanes. As the cells are given opportunity to select multiple biomolecule confronting them, the model serves as tool that can be used to study guidance and growth promotion/inhibition of proteins on cells.

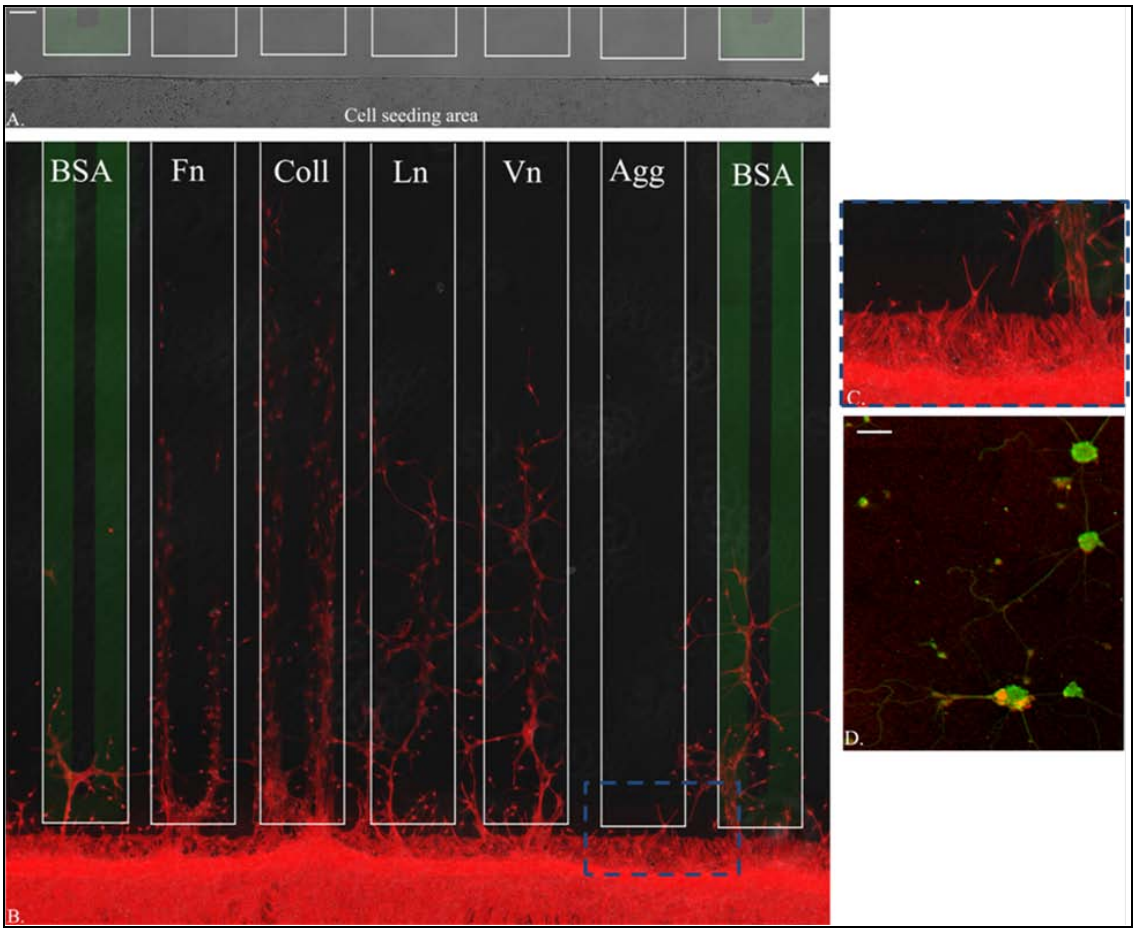

Figure 3.4 Cortical neurons seeded in 7-lane multi-biomolecule device. (A) Image showing the alignment of cortical neurons after pealing the device off. (B) Image showing the migration of cortical neurons (β-III tubulin – red) towards proteins in lanes. (C) Inset showing inhibition due to aggrecan lane. (D) Growth of E-18 cortical neurons (green) seeded on top of aggrecan (red). Scale bar 100 µm.

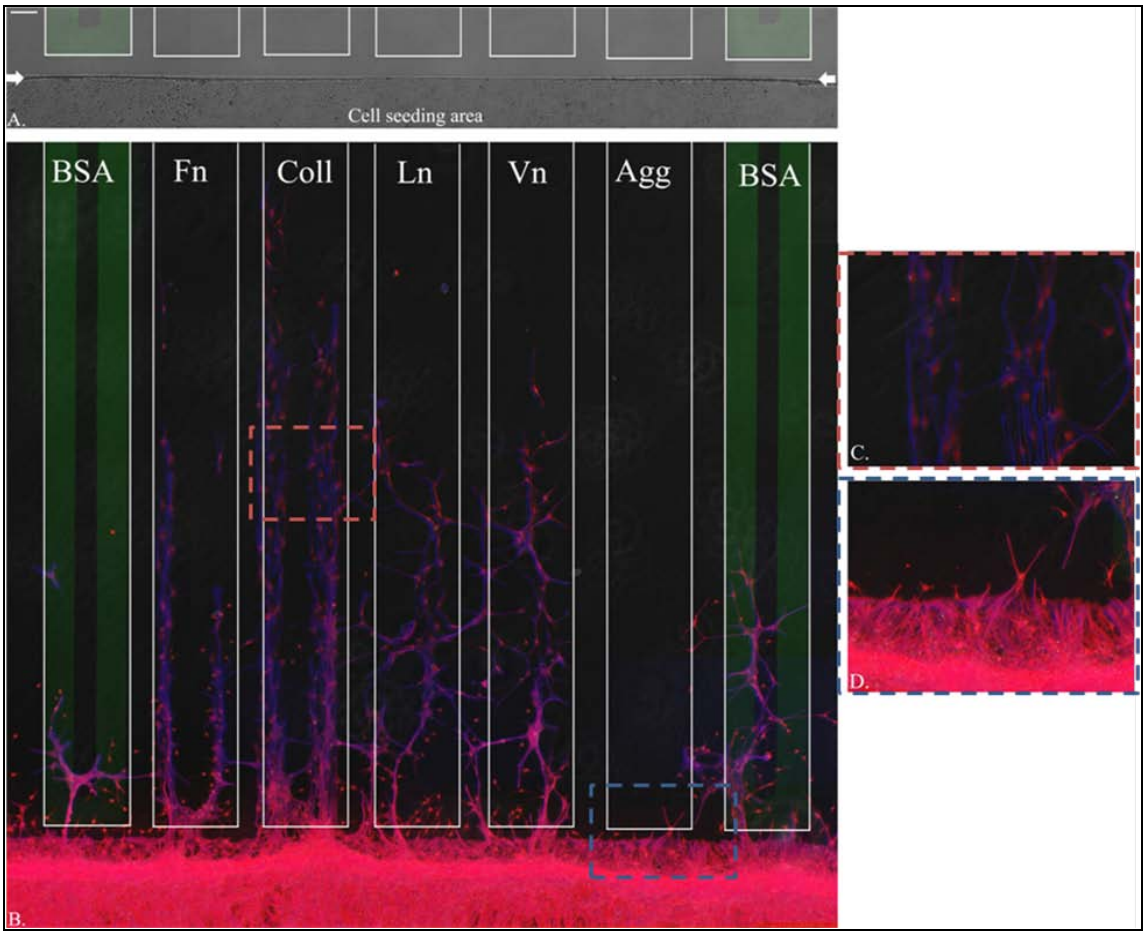

Figure 3.5 E-18 cortical neuron (red) migration stained for astrocytes (blue). (A) Initial image after device lift-off showing cell alignment. (B) Cell migration towards multiple proteins. (C) Inset showing co-localization of axons and astrocytes during migration. (D) Inset showing inhibition of axons and astrocytes by aggrecan. Scale bar 100 µm.

3.8.2 DRG migration study

E-18 derived DRG and Schwann cells were collected as described in section 3.6. Cell seeding area was coated with collagen type 1 to enhanced cell adhesion and growth of DRG neurons and Schwann cells. NBM + B-27 with BDNF and NT-3 as growth factors were used for cell culture. After the cell sprouting and accumulation near the PDMS barrier, the microfluidic device was lifted for the cells to migrate towards the adsorbed proteins in the lanes. Once the cells grew over the lanes, they were fixed using 4% paraformaldehyde and stained with β-III tubulin for axons and S-100 for Schwann cells for studying the growth and migration.

The DRG neurons and Schwann cells showed migration towards the laminin, fibronectin and collagen type 1 as compared to the rest of the proteins present in the adjacent lanes as seen in figure 3.6. Collagen type 1 showed a robust growth and faster rate of migration as compared to the adjacent proteins. This shows that the three proteins have a significant growth promoting effect on DRG neurons and Schwann cell culture and could play a vital role during development and regeneration of sensory neurons.

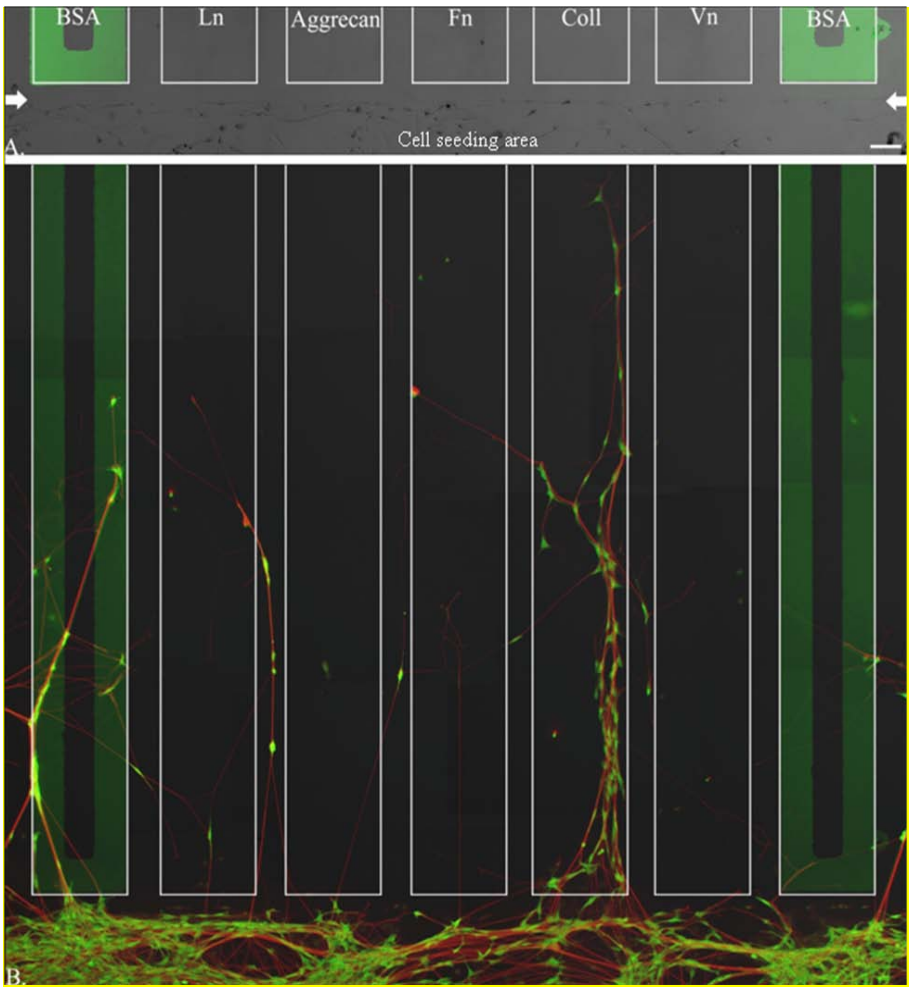

Figure 3.6 E-18 DRG axons (red) and Schwann cells (green) migrating towards multiple proteins. (A) Initial image after device life-off. (B) 60 hr after device lift-off. Scale bar 100 µm.

3.8.3 hGBM Migration Study

Primary hGBM cells were dissociated and 30,000 cells were seeded as described in section 3.7. The Petri dish substrate was pretreated with BSA (50 µg/ml) for initial cell adhesion followed by device assembly and protein coating inside the lanes. Once the cell attached and extended processes, the device was removed and the cells were allowed to migrate towards the protein lanes.

The hGBM cells showed a robust growth on the Laminin coated lane and some growth was observed towards fibronectin, collagen type 1 and BSA. The other protein lanes did not support sufficient cell growth as seen in figure 3.7. Laminin has a growth promoting effect and helps in radial cell migration of GBM can be seen from the technique mentioned in this study.

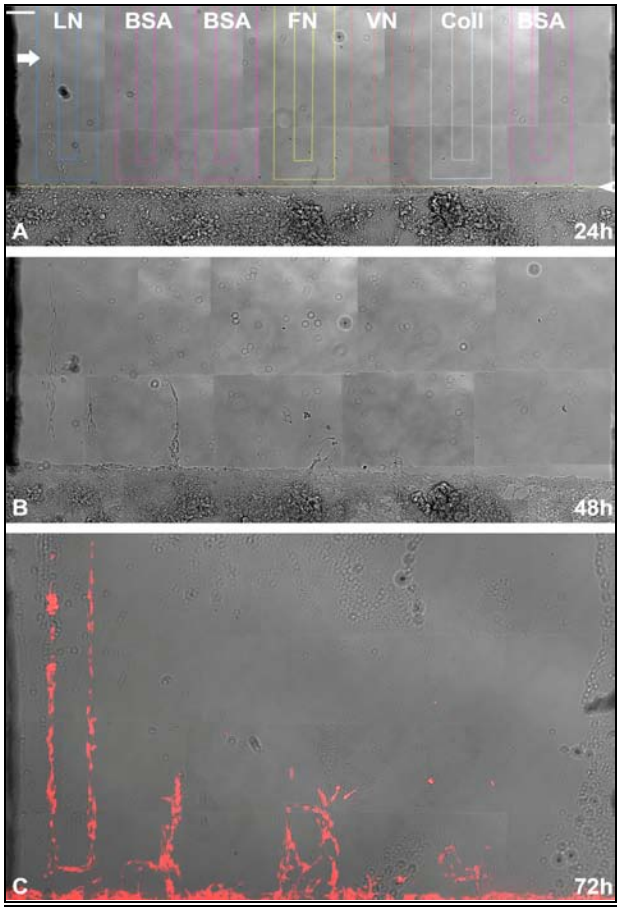

Figure 3.7 hGBM cell migration towards protein lanes. Scale bar 100 µm.

3.8.4 Effects of PDMS on Cells and Substrate

It was noticed that the substrate showed hydrophobicity where it came in contact with PDMS. An inhibitory effect of the microfluidic device on the cells after the device was pealed-off was noticed. With time, the cells could break through the barrier thus formed and reach the protein lanes. To overcome this issue, the PDMS was pretreated with PDL but it did not improve the outcome. It was also found that pre-treatment with PDL can form an irreversible bond when placed on a PDL coated substrate.

3.9 Conclusion

A new platform for studying the growth promoting and inhibiting effects of multiple proteins has been demonstrated here. We have also shown that the technique is unbiased and the effect of protein changes depending upon seeding on top or confrontation using aggrecan. We have demonstrated that the platform presented here can be used to study the cell-biomolecule interaction up to 20 biomolecules as compared to current method of 2 biomolecules at a time. This can not only be used to study cell migration in an unbiased manner, but also can be to form alternate stripes of proteins and study cell growth/inhibition by seeding cells on top like in stripe assays designed by F. Bonhoeffer and co-workers [53, 57].

CHAPTER 4

NOVEL MICROCHANNEL DEVICE – DESING AND WORKING

4.1 Dimensions of microchannel device

There are two designs that were made using PDMS to study the cell migration with respect to space. The devices have channels with a height of 15 µm and reservoirs at the height of 100 µm. the circular reservoir are connected to the cell seeding reservoirs by a 2 X 2 mm bridge for changing the medium without disturbing the cells. The channel length is 580 µm the distance between adjacent channels is 50 µm. The taper design is shown in figure 4.1.

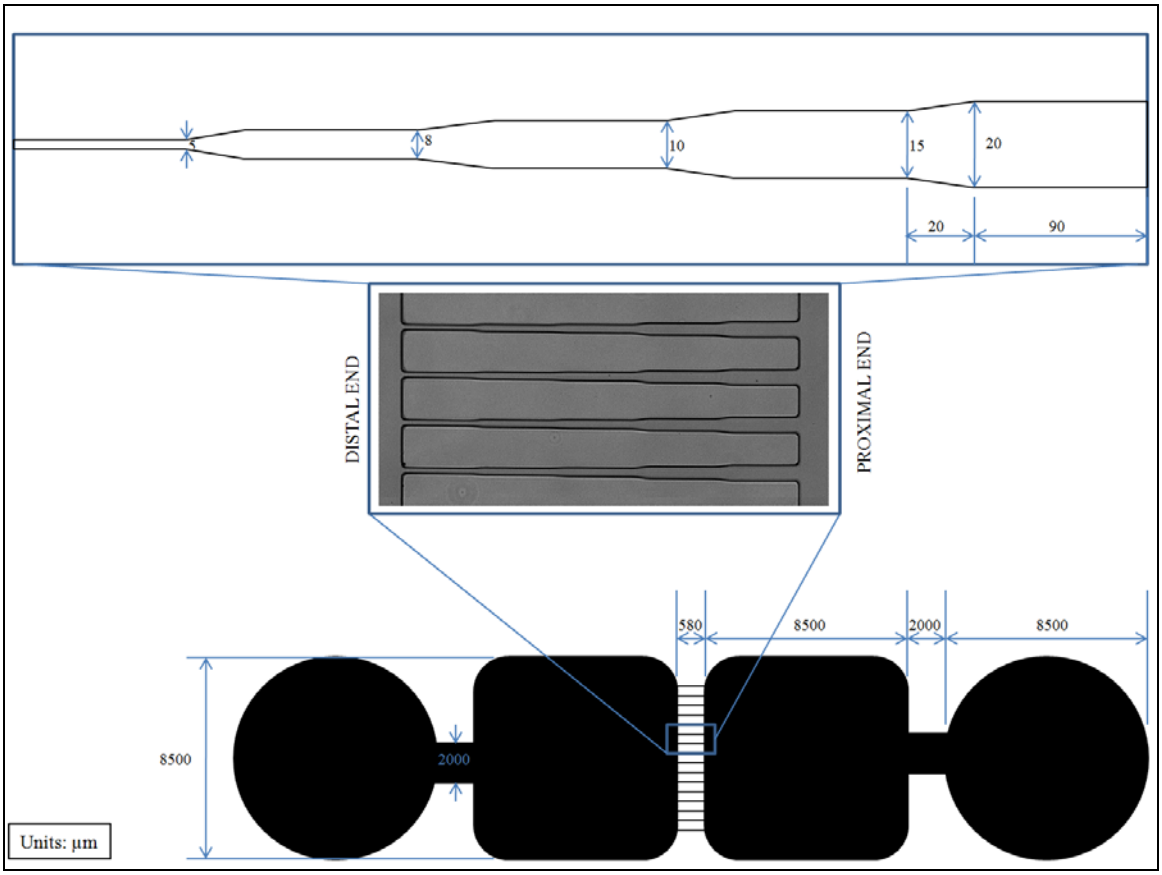

Figure 4.1 Schematics of novel microchannel device – taper design.

Figure 4.2 shows the multichannel design, channels with different dimension (5 µm, 8 µm, 10 µm, 15 µm and 20 µm) placed adjacent to each other. This helps in studying the migration of cells in a particular space over longer distance.

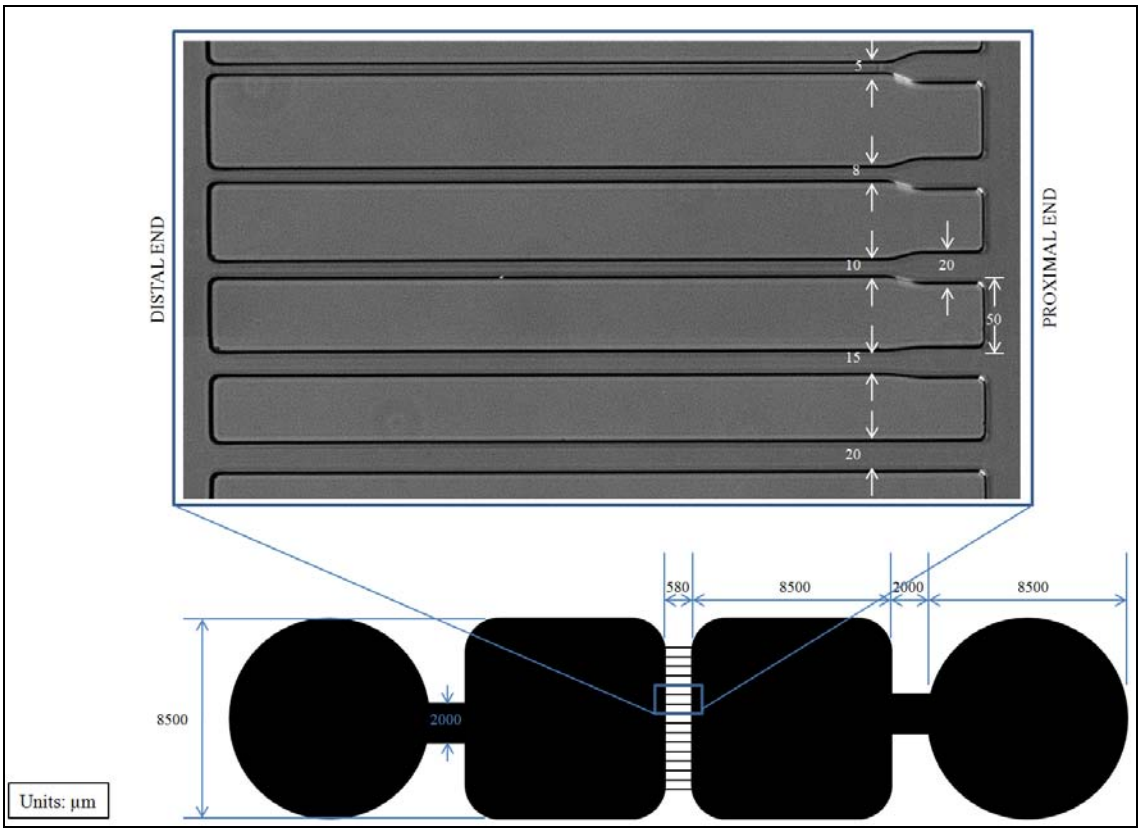

Figure 4.2 Schematic of novel microchannel device – multichannel design.

4.2 Device preparation and working

The microfluidic devices were fabricated as mentioned in Chapter 2. Briefly, for obtaining master mold, two layer photolithography processes were used. The first layer consisted of channels of taper design and multichannel design. SU-8 5 was spin coated to obtain a height of 15 µm exposed to UV to form the first layer. The second layer consisting of reservoirs 100 µm were formed by spin coating SU-8 50 on top of the channel containing wafer and exposing to UV. The two layers were overlapped for connecting the channels and reservoirs.

The PDMS based microfluidic devices thus formed were punched open with 8 mm tissue biopsy punches to form the reservoirs. Devices were cleaned using clear tape to remove PDMS debris followed by sterilization with 70% Ethanol for 25 minutes and DI water wash three times with 10 minute time intervals. Devices were air dried inside a biosafety cabinet. The dry devices were treated with oxygen plasma (pattern side facing up) for 30 minutes to make the PDMS hydrophilic and placed on sterilized glass coverslips. 1X PBS was added in the proximal end reservoirs and allowed to fill the channels followed by adding 1X PBS at the distal end reservoir. This made the device filled with fluid and ready to be used for protein coating.

For the migration study using hGBM cells, the device substrate was coated with laminin (10 µg/ml). Laminin expression is found to increase in the brain during glial brain tumors and promotes their radial migration [34, 93]. Expression of laminin was seen in cultures of E-18 cortical neurons as shown in figure 4.3. hGBM cells were seeded on top of cortical neurons and the cells attached and showed growth.

1X PBS from the reservoirs was drawn out and 100 µl of laminin was added to all reservoirs and placed at 37 °C inside cell culture incubator for 4 hours. The Laminin was removed and washed with 1X PBS 4 times with 10 minute interval and the reservoirs were filled with 200 µl tumor medium per well containing mEGF as growth factor.

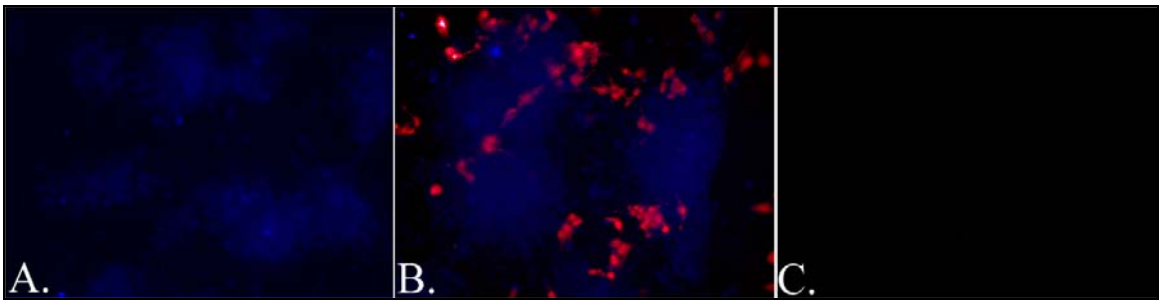

Figure 4.3 (A) Staining for laminin (blue) in E-18 derived cortical neuron culture. (B) hGBM (red) seeded on cortical neuron culture stained for laminin (blue) (C) Staining control.

4.3 Primary Glioblastoma Multiforme cell seeding

Primary human Glioblastoma Multiforme cells were obtained as mentioned before. 20 µl medium was taken from the proximal side reservoir and fed to the distal end reservoir before cell seeding. This helps to build a flow from the distal end reservoir to the proximal end and help prevent the cells from flowing to the distal end at the time of seeding. 30,000 /20 µl medium cells were seeded at proximal end reservoir by inserting the 200 µl pipette tip near the channels of the device. This results in alignment of the cells as close as possible to the microchannels. The cells were then followed as they migrate via the microchannels.

4.4 Cell migration study using taper design

This device is used to study the migration of a single cell through different dimensions of the microchannels. The cells are seeded at the proximal end and are allowed to travel through the channels. Images are taken at fixed time intervals and the change in cell morphology is studied. Images were taken at 10X 1X magnification and 63X 1X magnification. This helps to understand how the cells can change the morphology with availability of space. The hGBM cells travel from one cerebral hemisphere to the other via corpus callosum which is in sub micron scale. This device shows the characteristics of GBM cells to change their morphology while migrating in narrow spaces.

4.5 Cell Migration study using multichannel design

Cells were seeded in the proximal side reservoir and time point images were taken while the cells travel towards the distal end. Using multichannel design, the rate of migration of cell with respect to space can be calculated. The channels at the proximal side have an entry point which 50 µm wide to facilitate the cell migration initially. During the course of migration, images are taken at fixed time intervals to study rate of migration.

4.6 Results and Discussion

To measure the obtained dimension of microchannels, 5 different samples were used. Microchannels were imaged and using ImageJ, the width of channels was calculated. The

results are shown in table 4.1. There was an offset from the expected dimension due to variation in the exposure energy every time the devices were fabricated.

Table 4.1 Microchannel width of devices

Expected Dimension (µm)	Taper design Obtained dimension (µm)	Multichannel design Obtained dimension (µm)
5	5.43 ± 0.15	5.12 ± 0.19
8	8.38 ± 0.15	8.34 ± 0.22
10	10.52 ± 0.19	10.29 ± 0.14
15	14.97 ± 0.11	14.89 ± 0.28
20	19.99 ± 0.19	20.23 ± 0.35

4.6.1 Cell migration study using taper design

The study involved had n=4. It was found using the taper design that the cells were capable of squeezing themselves through to the distal side reservoir via the 5 µm channel. Figure 4.3 shows the migration of one hGBM cell passing from the proximal end reservoir to the distal end though the taper design. The cell moved freely through the 20 µm and 15 µm area and the cell size had reduced to pass through 10 µm, 8 µm and 5 µm. hGBM increased cell size at the end of the 5 µm channel showing the capability of the hGBM cell to change its morphology according to the availability of space. Due to this characteristic nature of hGBM cells, they migrate inside the brain and recurrence is seen after treatment. This device cannot be used to study the rate of cell migration as the channels of particular dimension are short and cells take longer time in transition between channel dimensions. Thus, the multichannel design helps in studying the rate of cell migration through a particular dimension.

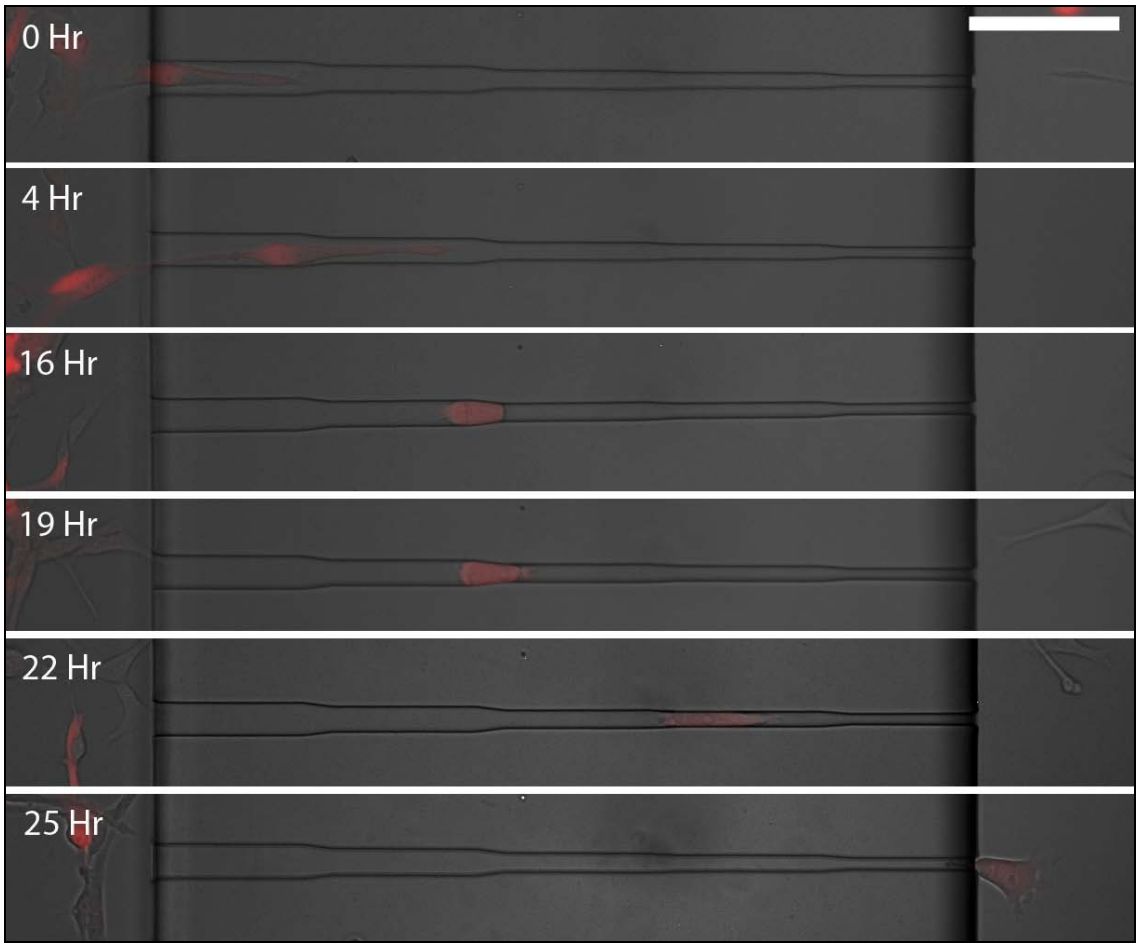

Figure 4.4 Image of taper design microchannels showing single hGBM cell migrating from proximal end to the distal end of the microchannel. Scale bar 100 µm.

Images of hGBM migration through the taper design were taken using 63X 1X oil emulsion lens. The cell processes were seen at this high magnification and it was seen that there were multiple cells inside the 5 µm channel coming out together to the distal end reservoir. This shows that the cells could work in synchrony even at very small spaces as seen in figure 4.4. The cells migrated from the 8 µm channel to the 5 µm channel and recovered back to normal size when they came out of the channel to the distal end reservoir. Figure 4.4 A – L shows the whole migration process and recovery of GBM cells.

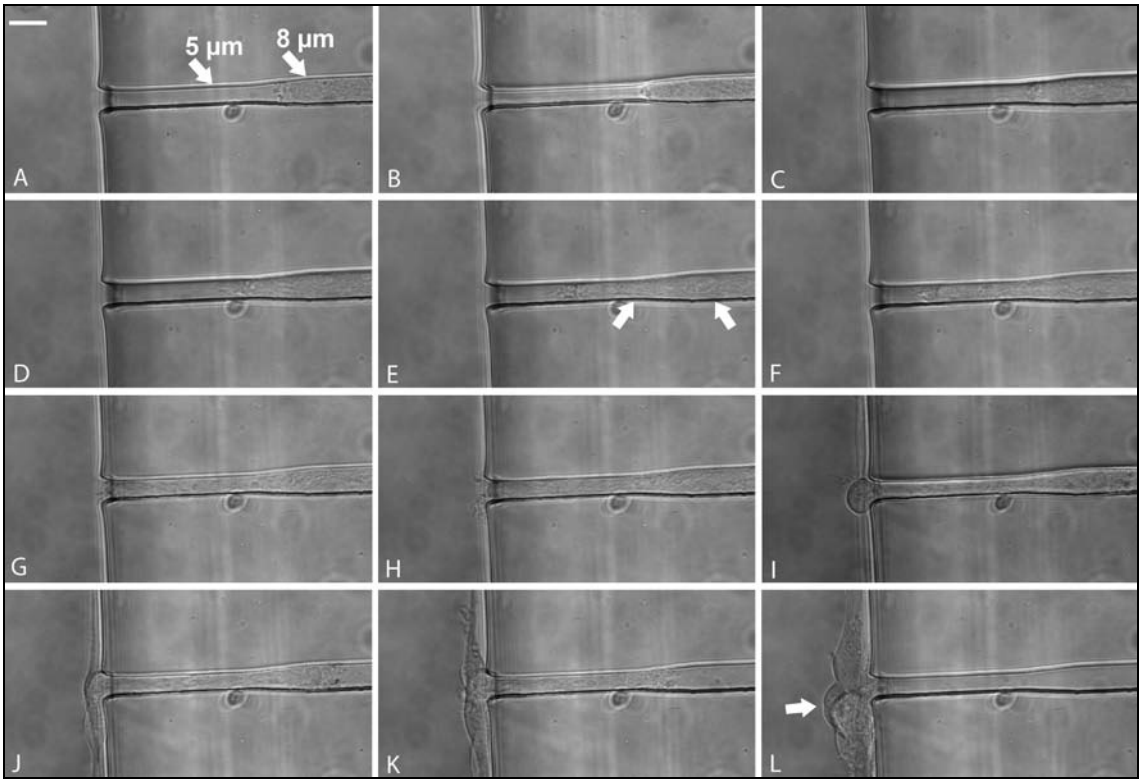

Figure 4.5 Migration of multiple cells from 8 µm to 5 µm and coming out at the distal end reservoir. (A) Showing cell migrating from 8 µm to 5 µm. (E) Multiple nuclei are seen inside the channels indicating the presence of multiple cells. (I) Cell body coming out and increasing size. (L) Image showing the size recovery after they come out of the 5 µm channel. Scale bar 10 µm.

In figure 4.5, three cells migrating towards the 10 µm channel from the 15 µm channel were seen to move together. The cells were connected by processes and when one cell migrated back towards the proximal reservoir, the process disconnected and over a period, the other two cells followed back to the proximal end reservoir. The image shows a process that is cut off over time and after which the migration of the cell towards the distal end reservoir was not seen. After some time, the cells start moving towards proximal end reservoir. Area of the two cells considering only the cell bodies was calculated in pixels using ImageJ. During the migration, the combined area of both the cells went down by 46%. This was calculated from the maximum (figure 4.5 C) area to the minimum area (figure 4.5 F) of cells shown by arrows in figure 4.5 C.

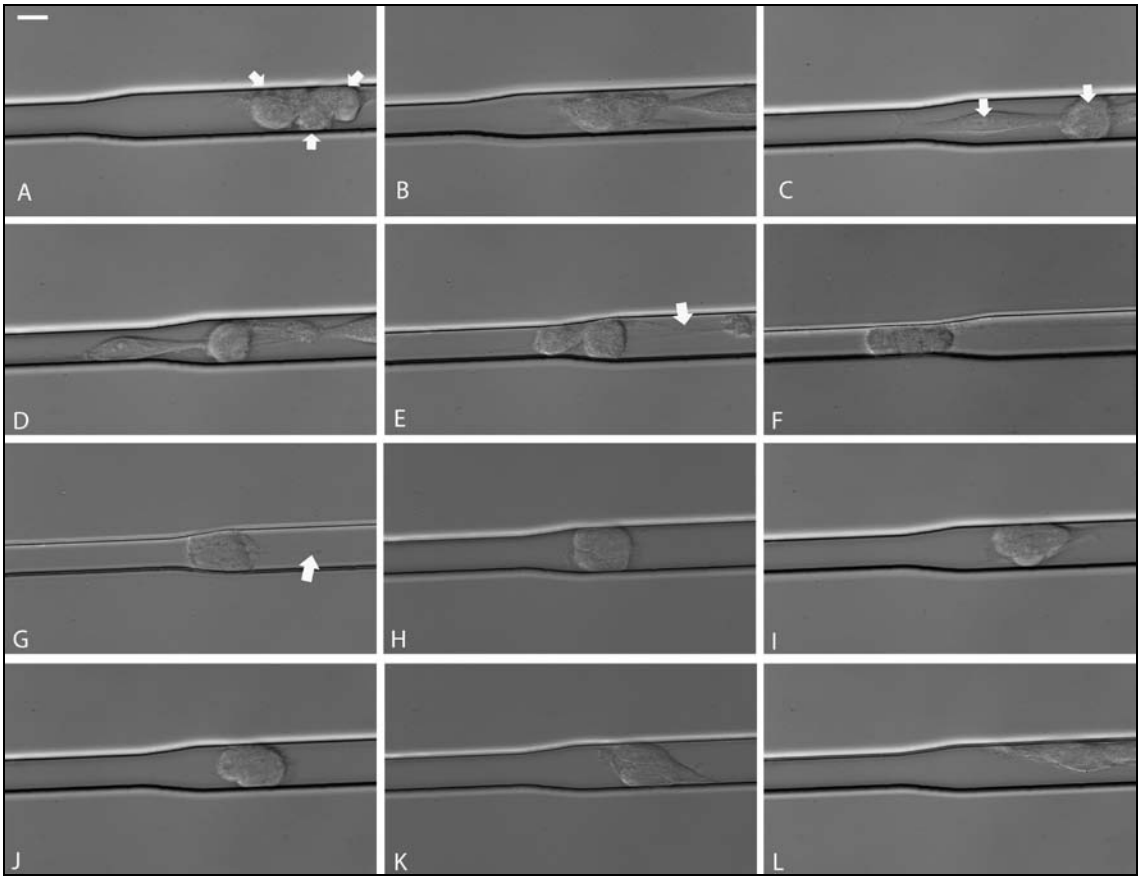

Figure 4.6 Image showing 3 cells migrating from 15 µm to 10 µm channel. (C) Shows the two cells that were considered for area calculation. The cells had the maximum area in this image and minimum in (F). (E) Image of process that connected the cells. (G) Shows the retraction of process. (L) Migration of the two cells back to the proximal side reservoir after the cell process retraction. Scale bar 10 µm.

4.6.2 Cell migration study using multichannel design

The multichannel device consisting of different dimensions of channels placed adjacent to each other was used to quantification of migration rate (n=4). The migration rate was calculated for single cells with respect to movement of cell body per hour. Figure 4.6 – 4.10 show the images of cell migrating through different channel width from proximal side to the distal side reservoir. The migration rate could not be calculated in 20 µm channel as the cells travelled in clusters.

Elastic modulus of the PDMS (1:10 ratio of curing agent: PDMS) used here is 1.783±0.177 MPa [94] whereas the effective shear modulus of human brain tissue *in vivo,* observed using magnetic resonance elastography is in the range of 5.2 -13.6 KPa [95-97]. During the course of migration, hGBM cells tend to reduce their size and also exert deforming pressure on the walls of PDMS as seen in figure 4.6 and 4.11. This shows that the cells can not only change their morphology, but also displace the surrounding brain tissue *in vivo* during migration through narrow spaces. It has been demonstrated that the structure, proliferation and migration of glioma cells are affected by the stiffness of substrate [98].

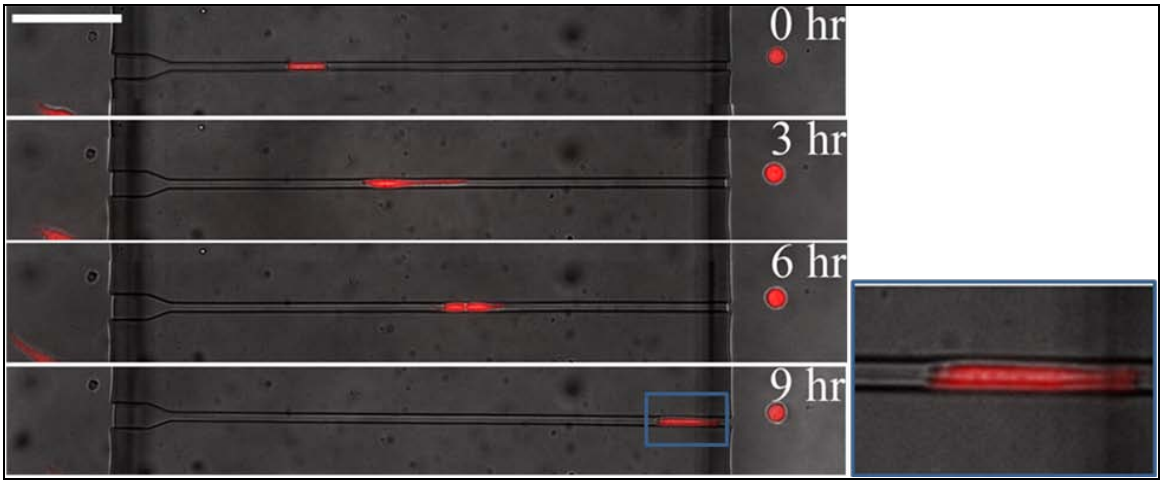

Figure 4.7 hGBM cell migration through 5 µm channel. Scale bar 100 µm.

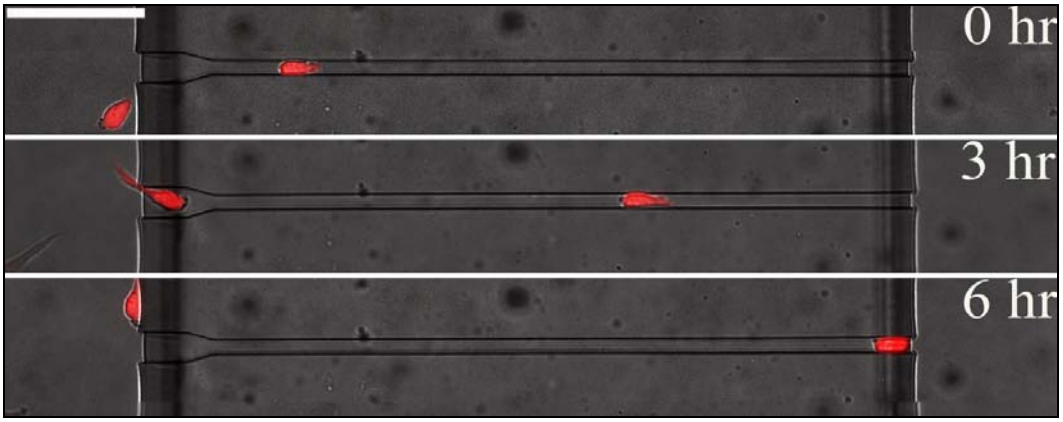

Figure 4.8 hGBM cell migration through 8 µm channel. Scale bar 100 µm.

Figure 4.9 hGBM cell migration through 10 µm channel. Scale bar 100 µm.

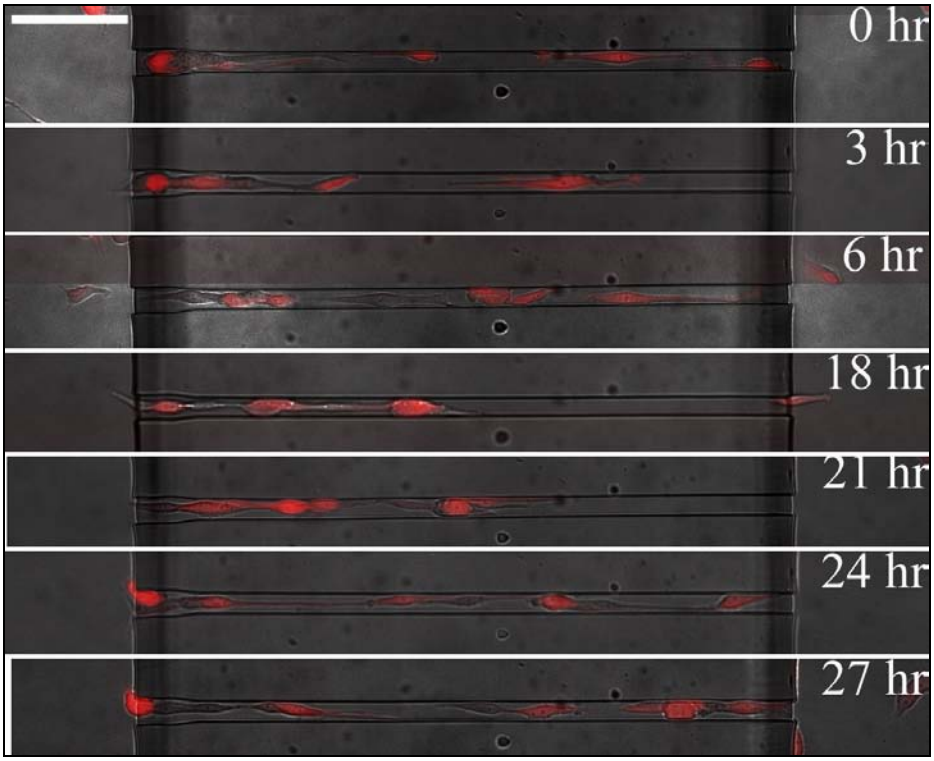

Figure 4.10 hGBM cell migration through 15 µm channel. Scale bar 100 µm.

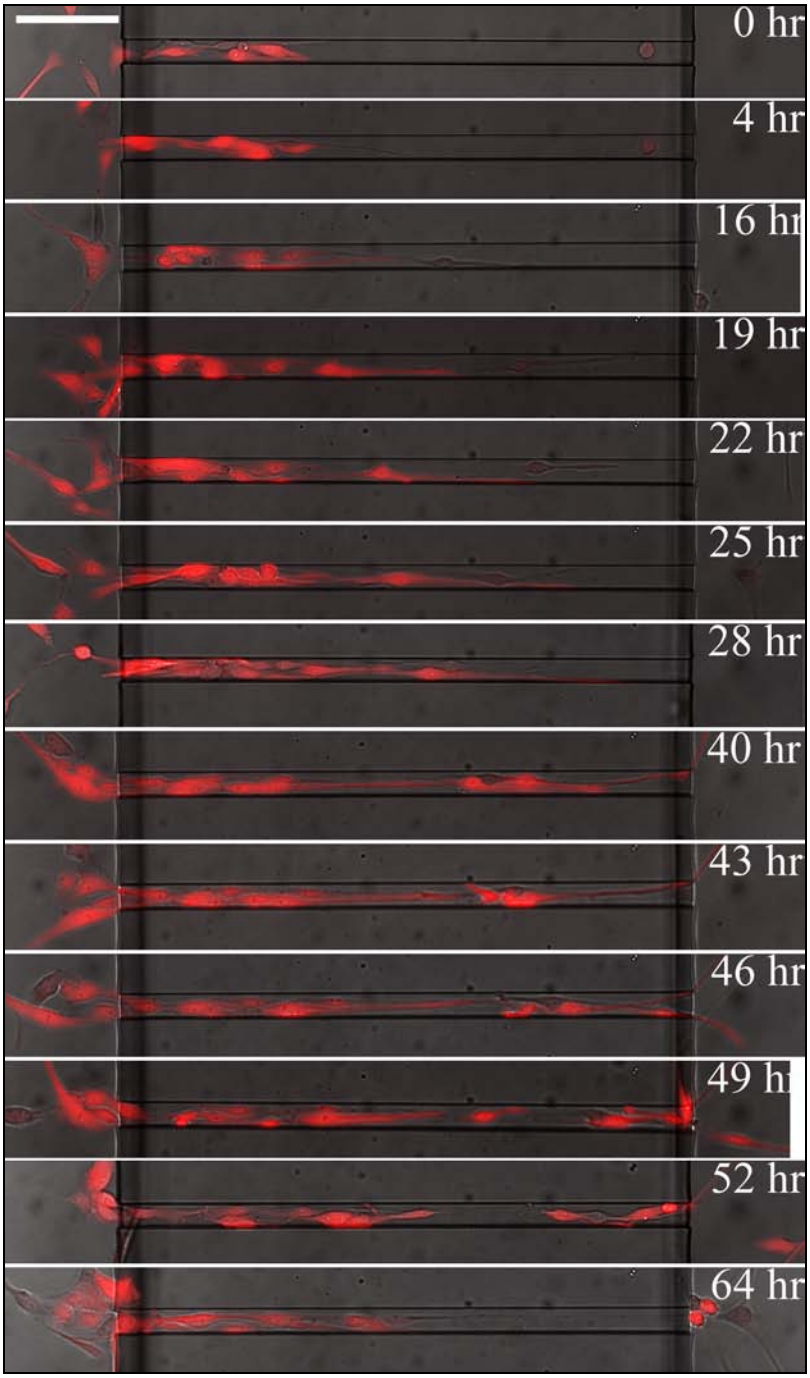

Figure 4.11 hGBM cell migration through 20 µm channel. Scale bar 100 µm.

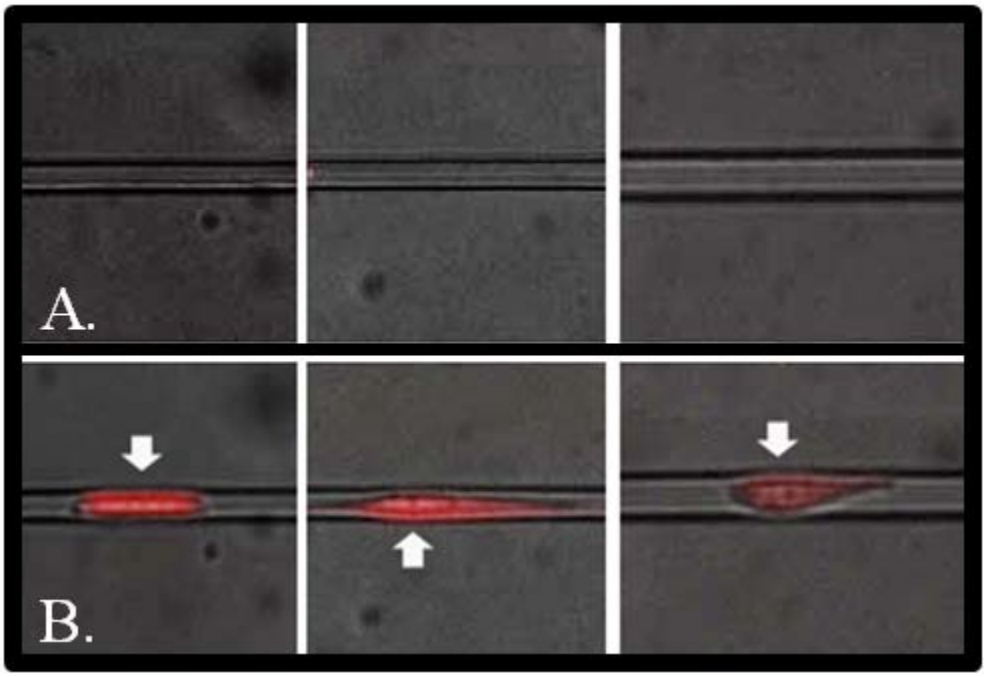

Figure 4.12 Image showing deformation of PDMS during cell migration. (A) PDMS channels before cell migration. (B) Arrows showing deformation during active cell migration.

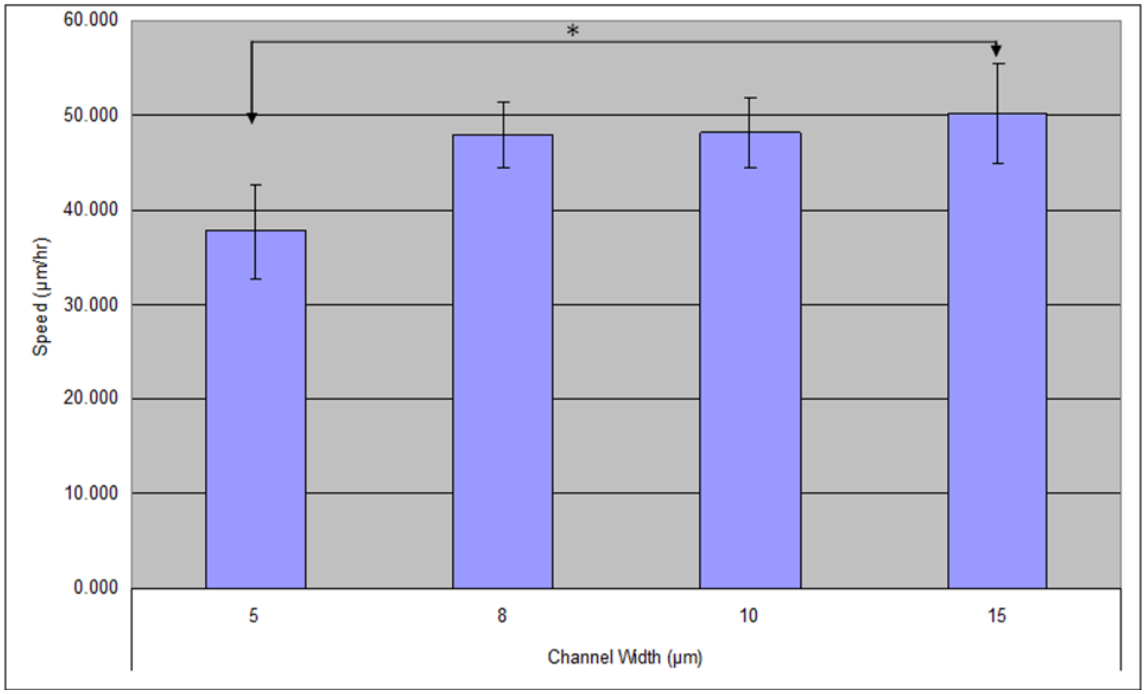

Figure 4.13 Migration rate (µm/hr) of cells through different channel width. *P<0.05.

For data analysis, ANOVA tukey was used between migration rate and channel width ($\alpha = 0.05$). There was a significant difference in migration rate between 5 µm and 15 µm channels. This shows that the migration rate of the cells is dependent on the availability of space. Rate of migration can be used to interpret the capability of the cells to undergo morphological changes and migrate in narrow spaces as seen as seen *in vivo.*

4.7 Conclusion

We have demonstrated a device that can be used to study the cell migration with respect to space. The platform allows visualization of live cell migration over distance which is restricted in current techniques like Boyden's chamber assay. The hGBM cells rarely metastasize into the blood stream and migrate inside the CNS in narrow space constrictions, thus KV chamber is a right model for the study. The device imparts knowledge on the reorganization of cell cytoskeleton and shear force imparted by the cell on surrounding tissues in the process of migration. This platform can not only be used to study the cell migration but also the taper design can be used to study interactions of two cells seeded on either sides of the channels. The channel size of 5 µm in the distal side prevents certain cells (Skeletal muscle cells) from moving into the channels froming a segregation. This device can be used to study the mechanisms of cancer cells that are exhibited during the process of metastasis. An *in vitro* platform to address the complex interactions occuring during the process of cell migration through narrow spaces has been demonstrated in this study.

CHAPTER 5

FUTURE WORK

Multi-Biomolecule will be used to study the cell-ECM interaction with different cells that metastasize to brain and will be compared with hGBM cells. This sort of study will enable us to study the different characteristic features of cancer cells in the CNS and will impart knowledge on better understanding of the hGBM cells. A combination of growth factors will be used to override the inhibitory effects of different molecules on neurons using this device.

The novel microchannel device will be used to culture cortical neurons on either sides of the channels to forms axonal network in the channels. The cortical neurons and the astrocytes move in a co-localized manner making the model of corpus callosum as seen in figure 5.1. Once a network of axons is formed, hGBM cells will be cultured on top and the mechanism of cell migration through corpus callosum will be studied. Different chemicals will be used to arrest the cell migration and chemotherapeutic drugs will be used to study the improvisation of the treatment outcome.

The Novel microchannel device will be used for studying the migration of renal cancer cells and lung cancer cells that metastasize to Brain. This will yield information on how much the cells can change their morphology in order to pass through space constrictions and how could they be prevented. By combining the results from multi-biomolecule device and novel multichannel device, restriction of hGBM cell migration will be studied and used *in vivo* for studying the efficiency.

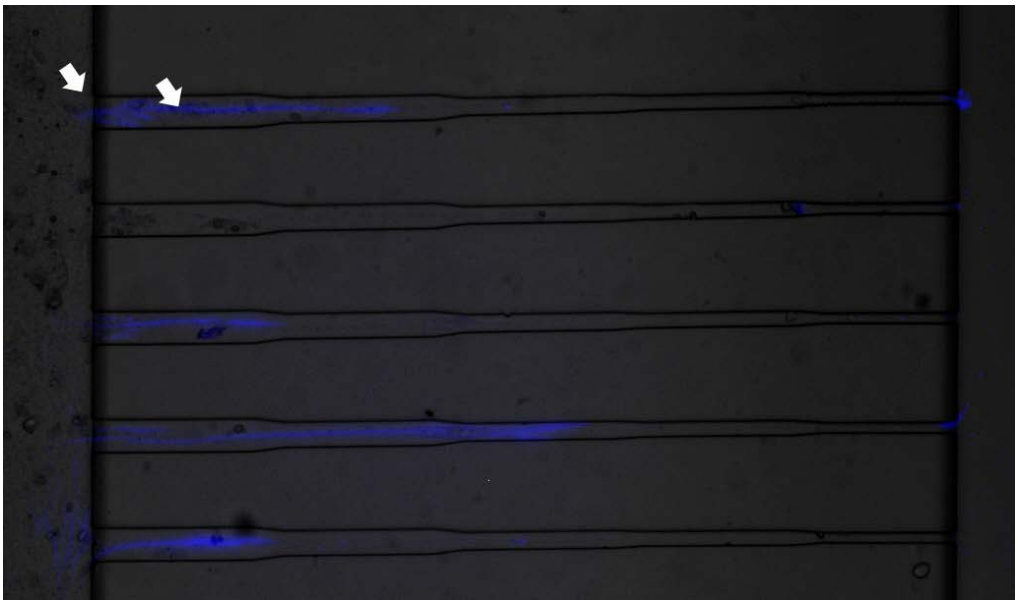

Figure 5.1 Cortical Neurons (White arrows) and Astrocyte (GFAP – Blue) travelling in channels.

REFERENCES

1. Beebe, D.J., Mensing, G.A. & Walker, G.M. Physics and applications of microfluidics in biology. *Annu Rev Biomed Eng* **4**, 261-86 (2002).
2. Mitchell, P. Microfluidics--downsizing large-scale biology. *Nat Biotechnol* **19**, 717-21 (2001).
3. Meldrum, D.R. & Holl, M.R. Tech.Sight. Microfluidics. Microscale bioanalytical systems. *Science* **297**, 1197-8 (2002).
4. Sia, S.K. & Whitesides, G.M. Microfluidic devices fabricated in poly(dimethylsiloxane) for biological studies. *Electrophoresis* **24**, 3563-76 (2003).
5. Lee, S.J. & Lee, S.Y. Micro total analysis system (micro-TAS) in biotechnology. *Appl Microbiol Biotechnol* **64**, 289-99 (2004).
6. Regehr, K.J. et al. Biological implications of polydimethylsiloxane-based microfluidic cell culture. *Lab Chip* **9**, 2132-9 (2009).
7. Taylor, A.M. et al. A microfluidic culture platform for CNS axonal injury, regeneration and transport. *Nat Methods* **2**, 599-605 (2005).
8. Kim, Y.T., Karthikeyan, K., Chirvi, S. & Dave, D.P. Neuro-optical microfluidic platform to study injury and regeneration of single axons. *Lab Chip* **9**, 2576-81 (2009).
9. Pinto, S. et al. Poly(dimethyl siloxane) surface modification by low pressure plasma to improve its characteristics towards biomedical applications. *Colloids Surf B Biointerfaces* (2010).
10. Alauzun, J.G. et al. Biocompatible, hyaluronic acid modified silicone elastomers. *Biomaterials* **31**, 3471-8 (2010).
11. Schneemilch, M. & Quirke, N. Effect of oxidation on the wettability of poly(dimethylsiloxane) surfaces. *J Chem Phys* **127**, 114701 (2007).
12. Zhou, J., Ellis, A.V. & Voelcker, N.H. Recent developments in PDMS surface modification for microfluidic devices. *Electrophoresis* **31**, 2-16 (2010).
13. McDonald, J.C. et al. Fabrication of microfluidic systems in poly(dimethylsiloxane). *Electrophoresis* **21**, 27-40 (2000).
14. Nie, F.Q. et al. On-chip cell migration assay using microfluidic channels. *Biomaterials* **28**, 4017-22 (2007).
15. Dertinger, S.K., Jiang, X., Li, Z., Murthy, V.N. & Whitesides, G.M. Gradients of substrate-bound laminin orient axonal specification of neurons. *Proc Natl Acad Sci U S A* **99**, 12542-7 (2002).
16. Vielmetter, J., Stolze, B., Bonhoeffer, F. & Stuermer, C.A. In vitro assay to test differential substrate affinities of growing axons and migratory cells. *Exp Brain Res* **81**, 283-7 (1990).
17. Reichardt, L.F. & Tomaselli, K.J. Extracellular matrix molecules and their receptors: functions in neural development. *Annu Rev Neurosci* **14**, 531-70 (1991).
18. Boiko, T. et al. Ankyrin-dependent and -independent mechanisms orchestrate axonal compartmentalization of L1 family members neurofascin and L1/neuron-glia cell adhesion molecule. *J Neurosci* **27**, 590-603 (2007).
19. Nadarajah, B. & Parnavelas, J.G. Modes of neuronal migration in the developing cerebral cortex. *Nat Rev Neurosci* **3**, 423-32 (2002).
20. Sobel, R.A. The extracellular matrix in multiple sclerosis: an update. *Braz J Med Biol Res* **34**, 603-9 (2001).
21. Jones, L.S. Integrins: possible functions in the adult CNS. *Trends Neurosci* **19**, 68-72 (1996).

22. Zimmermann, D.R. & Dours-Zimmermann, M.T. Extracellular matrix of the central nervous system: from neglect to challenge. *Histochem Cell Biol* **130**, 635-53 (2008).
23. Sanes, J.R. Extracellular matrix molecules that influence neural development. *Annu Rev Neurosci* **12**, 491-516 (1989).
24. Rosso, F., Giordano, A., Barbarisi, M. & Barbarisi, A. From cell-ECM interactions to tissue engineering. *J Cell Physiol* **199**, 174-80 (2004).
25. Armstrong, S.J., Wiberg, M., Terenghi, G. & Kingham, P.J. ECM molecules mediate both Schwann cell proliferation and activation to enhance neurite outgrowth. *Tissue Eng* **13**, 2863-70 (2007).
26. Kearns, S.M., Laywell, E.D., Kukekov, V.K. & Steindler, D.A. Extracellular matrix effects on neurosphere cell motility. *Exp Neurol* **182**, 240-4 (2003).
27. Venstrom, K.A. & Reichardt, L.F. Extracellular matrix. 2: Role of extracellular matrix molecules and their receptors in the nervous system. *Faseb J* **7**, 996-1003 (1993).
28. O'Connor, T.P. & Bentley, D. Accumulation of actin in subsets of pioneer growth cone filopodia in response to neural and epithelial guidance cues in situ. *J Cell Biol* **123**, 935-48 (1993).
29. Schmidt, C.E., Dai, J., Lauffenburger, D.A., Sheetz, M.P. & Horwitz, A.F. Integrin-cytoskeletal interactions in neuronal growth cones. *J Neurosci* **15**, 3400-7 (1995).
30. Stetler-Stevenson, W.G., Aznavoorian, S. & Liotta, L.A. Tumor cell interactions with the extracellular matrix during invasion and metastasis. *Annu Rev Cell Biol* **9**, 541-73 (1993).
31. Lukashev, M.E. & Werb, Z. ECM signalling: orchestrating cell behaviour and misbehaviour. *Trends Cell Biol* **8**, 437-41 (1998).
32. Friedlander, D.R. et al. Migration of brain tumor cells on extracellular matrix proteins in vitro correlates with tumor type and grade and involves alphaV and beta1 integrins. *Cancer Res* **56**, 1939-47 (1996).
33. Lefranc, F., Rynkowski, M., DeWitte, O. & Kiss, R. Present and potential future adjuvant issues in high-grade astrocytic glioma treatment. *Adv Tech Stand Neurosurg* **34**, 3-35 (2009).
34. Demuth, T. & Berens, M.E. Molecular mechanisms of glioma cell migration and invasion. *J Neurooncol* **70**, 217-28 (2004).
35. Friedl, P. & Wolf, K. Tumour-cell invasion and migration: diversity and escape mechanisms. *Nat Rev Cancer* **3**, 362-74 (2003).
36. Robins, H.I., Chang, S., Butowski, N. & Mehta, M. Therapeutic advances for glioblastoma multiforme: current status and future prospects. *Curr Oncol Rep* **9**, 66-70 (2007).
37. Groves, M.D. et al. A North American brain tumor consortium (NABTC 99-04) phase II trial of temozolomide plus thalidomide for recurrent glioblastoma multiforme. *J Neurooncol* **81**, 271-7 (2007).
38. Kanu, O.O. et al. Glioblastoma Multiforme Oncogenomics and Signaling Pathways. *Clin Med Oncol* **3**, 39-52 (2009).
39. Nakada, M. et al. The phosphorylation of ephrin-B2 ligand promotes glioma cell migration and invasion. *Int J Cancer* **126**, 1155-65 (2010).
40. Giese, A., Bjerkvig, R., Berens, M.E. & Westphal, M. Cost of migration: invasion of malignant gliomas and implications for treatment. *J Clin Oncol* **21**, 1624-36 (2003).
41. Bello, L. et al. Combinatorial administration of molecules that simultaneously inhibit angiogenesis and invasion leads to increased therapeutic efficacy in mouse models of malignant glioma. *Clin Cancer Res* **10**, 4527-37 (2004).
42. Mourad, P.D., Farrell, L., Stamps, L.D., Chicoine, M.R. & Silbergeld, D.L. Why are systemic glioblastoma metastases rare? Systemic and cerebral growth of mouse glioblastoma. *Surg Neurol* **63**, 511-9; discussion 519 (2005).

43. Bernstein, J.J. & Woodard, C.A. Glioblastoma cells do not intravasate into blood vessels. *Neurosurgery* **36**, 124-32; discussion 132 (1995).
44. Uhm, J.H., Gladson, C.L. & Rao, J.S. The role of integrins in the malignant phenotype of gliomas. *Front Biosci* **4**, D188-99 (1999).
45. Giancotti, F.G. & Ruoslahti, E. Integrin signaling. *Science* **285**, 1028-32 (1999).
46. Jalali, S. et al. Integrin-mediated mechanotransduction requires its dynamic interaction with specific extracellular matrix (ECM) ligands. *Proc Natl Acad Sci U S A* **98**, 1042-6 (2001).
47. Rees, S., Cragg, B.G. & Everitt, A.V. Comparison of extracellular space in the mature and aging rat brain using a new technique. *J Neurol Sci* **53**, 347-57 (1982).
48. Frieboes, H.B. et al. An integrated computational/experimental model of tumor invasion. *Cancer Res* **66**, 1597-604 (2006).
49. Andersson, H. & van den Berg, A. Microfabrication and microfluidics for tissue engineering: state of the art and future opportunities. *Lab Chip* **4**, 98-103 (2004).
50. Desai, T.A. Micro- and nanoscale structures for tissue engineering constructs. *Med Eng Phys* **22**, 595-606 (2000).
51. Rolli, C.G., Seufferlein, T., Kemkemer, R. & Spatz, J.P. Impact of tumor cell cytoskeleton organization on invasiveness and migration: a microchannel-based approach. *PLoS One* **5**, e8726 (2010).
52. Flemming, R.G., Murphy, C.J., Abrams, G.A., Goodman, S.L. & Nealey, P.F. Effects of synthetic micro- and nano-structured surfaces on cell behavior. *Biomaterials* **20**, 573-88 (1999).
53. Walter, J., Kern-Veits, B., Huf, J., Stolze, B. & Bonhoeffer, F. Recognition of position-specific properties of tectal cell membranes by retinal axons in vitro. *Development* **101**, 685-96 (1987).
54. Mann, F., Zhukareva, V., Pimenta, A., Levitt, P. & Bolz, J. Membrane-associated molecules guide limbic and nonlimbic thalamocortical projections. *J Neurosci* **18**, 9409-19 (1998).
55. Calof, A.L., Campanero, M.R., O'Rear, J.J., Yurchenco, P.D. & Lander, A.D. Domain-specific activation of neuronal migration and neurite outgrowth-promoting activities of laminin. *Neuron* **13**, 117-30 (1994).
56. Walter, J., Muller, B. & Bonhoeffer, F. Axonal guidance by an avoidance mechanism. *J Physiol (Paris)* **84**, 104-10 (1990).
57. Walter, J., Henke-Fahle, S. & Bonhoeffer, F. Avoidance of posterior tectal membranes by temporal retinal axons. *Development* **101**, 909-13 (1987).
58. Feldheim, D.A. et al. Genetic analysis of ephrin-A2 and ephrin-A5 shows their requirement in multiple aspects of retinocollicular mapping. *Neuron* **25**, 563-74 (2000).
59. Drescher, U. et al. In vitro guidance of retinal ganglion cell axons by RAGS, a 25 kDa tectal protein related to ligands for Eph receptor tyrosine kinases. *Cell* **82**, 359-70 (1995).
60. Knoll, B., Weinl, C., Nordheim, A. & Bonhoeffer, F. Stripe assay to examine axonal guidance and cell migration. *Nat Protoc* **2**, 1216-24 (2007).
61. Hodgkinson, G.N., Tresco, P.A. & Hlady, V. The differential influence of colocalized and segregated dual protein signals on neurite outgrowth on surfaces. *Biomaterials* **28**, 2590-602 (2007).
62. Blesch, A. & Tuszynski, M.H. Spinal cord injury: plasticity, regeneration and the challenge of translational drug development. *Trends Neurosci* **32**, 41-7 (2009).
63. Chung, S., Sudo, R., Vickerman, V., Zervantonakis, I.K. & Kamm, R.D. Microfluidic Platforms for Studies of Angiogenesis, Cell Migration, and Cell-Cell Interactions : Sixth International Bio-Fluid Mechanics Symposium and Workshop March 28-30, 2008 Pasadena, California. *Ann Biomed Eng* (2010).

64. Frisk, T. et al. A microfluidic device for parallel 3-D cell cultures in asymmetric environments. *Electrophoresis* **28**, 4705-12 (2007).
65. Chen, H.C. Boyden chamber assay. *Methods Mol Biol* **294**, 15-22 (2005).
66. Kleinman, H.K. & Jacob, K. Invasion assays. *Curr Protoc Cell Biol* **Chapter 12**, Unit 12 2 (2001).
67. Rockne, R. et al. Predicting the efficacy of radiotherapy in individual glioblastoma patients in vivo: a mathematical modeling approach. *Phys Med Biol* **55**, 3271-85 (2010).
68. Harpold, H.L., Alvord, E.C., Jr. & Swanson, K.R. The evolution of mathematical modeling of glioma proliferation and invasion. *J Neuropathol Exp Neurol* **66**, 1-9 (2007).
69. Jessen, K.R. & Mirsky, R. The origin and development of glial cells in peripheral nerves. *Nat Rev Neurosci* **6**, 671-82 (2005).
70. Vernadakis, A. & Roots, B.I. Neuron-glia interrelations during phylogeny (Humana Press, Totowa, N.J., 1995).
71. Lopez-Munoz, F., Boya, J. & Alamo, C. Neuron theory, the cornerstone of neuroscience, on the centenary of the Nobel Prize award to Santiago Ramon y Cajal. *Brain Res Bull* **70**, 391-405 (2006).
72. Jessen, K.R. Glial cells. *Int J Biochem Cell Biol* **36**, 1861-7 (2004).
73. Fix, J.D. & Brueckner, J.K. High yield neuroanatomy (Wolters Kluwer/Lippincott Williams & Wilkins, Philadelphia, 2009).
74. Angevine, J.B. & Cotman, C.W. Principles of neuroanatomy (Oxford University Press, New York, 1981).
75. Buonomano, D.V. & Merzenich, M.M. Cortical plasticity: from synapses to maps. *Annu Rev Neurosci* **21**, 149-86 (1998).
76. Martin, J.H. Neuroanatomy : text and atlas (McGraw-Hill, New York, N.Y., 2003).
77. Reavey-Cantwell, J.F. et al. The prognostic value of tumor markers in patients with glioblastoma multiforme: analysis of 32 patients and review of the literature. *J Neurooncol* **55**, 195-204 (2001).
78. Hou, L.C., Veeravagu, A., Hsu, A.R. & Tse, V.C. Recurrent glioblastoma multiforme: a review of natural history and management options. *Neurosurg Focus* **20**, E5 (2006).
79. Ziegler, D.S. et al. Resistance of human glioblastoma multiforme cells to growth factor inhibitors is overcome by blockade of inhibitor of apoptosis proteins. *J Clin Invest* **118**, 3109-22 (2008).
80. Markert, J. Glioblastoma Multiforme (Jones and Bartlett Publishers, Sudbury, Mass., 2005).
81. Yanamandra, N. et al. Blockade of cathepsin B expression in human glioblastoma cells is associated with suppression of angiogenesis. *Oncogene* **23**, 2224-30 (2004).
82. Senft, C. et al. Inhibition of the JAK-2/STAT3 signaling pathway impedes the migratory and invasive potential of human glioblastoma cells. *J Neurooncol* (2010).
83. Furnari, F.B. et al. Malignant astrocytic glioma: genetics, biology, and paths to treatment. *Genes Dev* **21**, 2683-710 (2007).
84. Kitange, G.J. et al. Expression of CD74 in high grade gliomas: a potential role in temozolomide resistance. *J Neurooncol* (2010).
85. Kitange, G.J. et al. Induction of MGMT expression is associated with temozolomide resistance in glioblastoma xenografts. *Neuro Oncol* **11**, 281-91 (2009).
86. Kitange, G.J. et al. Evaluation of MGMT promoter methylation status and correlation with temozolomide response in orthotopic glioblastoma xenograft model. *J Neurooncol* **92**, 23-31 (2009).
87. Ransom, C.B., O'Neal, J.T. & Sontheimer, H. Volume-activated chloride currents contribute to the resting conductance and invasive migration of human glioma cells. *J Neurosci* **21**, 7674-83 (2001).
88. Ullrich, N., Bordey, A., Gillespie, G.Y. & Sontheimer, H. Expression of voltage-activated chloride currents in acute slices of human gliomas. *Neuroscience* **83**, 1161-73 (1998).

89. Olsen, M.L., Schade, S., Lyons, S.A., Amaral, M.D. & Sontheimer, H. Expression of voltage-gated chloride channels in human glioma cells. *J Neurosci* **23**, 5572-82 (2003).
90. Soroceanu, L., Manning, T.J., Jr. & Sontheimer, H. Modulation of glioma cell migration and invasion using Cl(-) and K(+) ion channel blockers. *J Neurosci* **19**, 5942-54 (1999).
91. Liang, Q.C. et al. Inhibition of transcription factor STAT5b suppresses proliferation, induces G1 cell cycle arrest and reduces tumor cell invasion in human glioblastoma multiforme cells. *Cancer Lett* **273**, 164-71 (2009).
92. Cheng, B. & Mattson, M.P. NT-3 and BDNF protect CNS neurons against metabolic/excitotoxic insults. *Brain Res* **640**, 56-67 (1994).
93. Ljubimova, J.Y., Fujita, M., Khazenzon, N.M., Ljubimov, A.V. & Black, K.L. Changes in laminin isoforms associated with brain tumor invasion and angiogenesis. *Front Biosci* **11**, 81-8 (2006).
94. Brown, X.Q., Ookawa, K. & Wong, J.Y. Evaluation of polydimethylsiloxane scaffolds with physiologically-relevant elastic moduli: interplay of substrate mechanics and surface chemistry effects on vascular smooth muscle cell response. *Biomaterials* **26**, 3123-9 (2005).
95. Mariappan, Y.K., Glaser, K.J. & Ehman, R.L. Magnetic resonance elastography: a review. *Clin Anat* **23**, 497-511 (2010).
96. Kruse, S.A. et al. Magnetic resonance elastography of the brain. *Neuroimage* **39**, 231-7 (2008).
97. McCracken, P.J., Manduca, A., Felmlee, J. & Ehman, R.L. Mechanical transient-based magnetic resonance elastography. *Magn Reson Med* **53**, 628-39 (2005).
98. Ulrich, T.A., de Juan Pardo, E.M. & Kumar, S. The mechanical rigidity of the extracellular matrix regulates the structure, motility, and proliferation of glioma cells. *Cancer Res* **69**, 4167-74 (2009).

BIOGRAPHICAL INFORMATION

Srikanth Vasudevan was born in Chennai, India on 4th of August 1984. He obtained his Bachelor's Degree in Biomedical Instrumentation from Dr. M.G.R. University, Chennai India in 2007 June. During Bachelor's Degree, he completed an Implant Training at Carl Zeiss India Ltd., in summer 2005. After course completion, he joined Indus Medical Instruments Pvt. Ltd as Regional Sale Specialist in March 2008 and worked till June 2008. After showing immense interest in research at work, he joined The University of Texas at Arlington in fall 2008 and joined Dr. Young-tae Kim's laboratory in November 2008 for pursuing research in the field of Neuroengineering. It is the ultimate aim of his life to contribute to the field of Neuroscience and Neuro-oncology for betterment of current treatment and improving the quality of life.